

Sharp \mathbf{k} -space features in the order parameter within the interlayer pair-tunneling mechanism of high- T_c superconductivity

Giuseppe G.N. Angilella, Renato Pucci, Fabio Siringo

Dipartimento di Fisica dell'Università di Catania,

and Istituto Nazionale per la Fisica della Materia, Unità di Ricerca di Catania,

57, Corso Italia, I-95129 Catania, Italy

Asle Sudbø

Institutt for Fysikk, Norges Teknisk-Naturvitenskapelige Universitetet,

Sem Sælandsvei 9, Gløshaugen, N-7034 Trondheim, Norway

(April 16, 1998; revised October 5, 1998)

We study the \mathbf{k} -dependence of the gap function of a bilayer superconductor, using standard mean-field techniques applied to a two-dimensional ($2D$) extended Hubbard model, in the presence of coherent interlayer pair-tunneling and quenched coherent single-particle tunneling. The *intralayer* pairing potential thus defined is expandable in a finite number (5) of basis functions for the irreducible representations of the point-group of the perfectly square lattice, C_{4v} . This gives rise to a competition between *s*- and *d*-wave symmetry, as the chemical potential is increased from the bottom to the top of a realistic band for most cuprates. It allows for mixed-symmetry paired state at temperatures below T_c , but never at T_c on a square lattice. Inclusion of the interlayer pair-tunneling into the effective pairing potential leads to highly non-trivial \mathbf{k} -space structures, such as pronounced maxima along the Fermi line not seen in the absence of interlayer pair-tunneling. We show how such a gap structure evolves with temperature and with band filling, and how it affects various observables. In particular, a nonuniversal value of the normalized jump in the specific heat at T_c will be evidenced, at variance with the conventional universal BCS result.

PACS numbers: 74.20.-z 74.80.Dm 74.72.Hs 74.25.Bt

I. INTRODUCTION

The identification of the character of the asymptotic low-energy excitations of the the high- T_c superconductors (HTCS) continues to present a formidable challenge to theorists and experimentalists in condensed matter physics. These excitations are presumably a key feature in understanding the basics of the phenomenon.¹ Although the superconducting state of the cuprates to a large extent in the recent past has been considered conventional, it is becoming increasingly clear that such a statement requires certain modifications, to say the least.² The latter statement is supported by recent experimental findings.^{3,4}

The controversy over the symmetry of the paired state (*s*- and extended *s*-wave vs higher order waves, particularly *d*-wave) and the coupling strength can nowadays be restated in more precise terms, due to the availability of samples with adequately pure composition and structure, and of improvements of experimental techniques. A central tool in this context is angle-resolved photoemission spectroscopy (ARPES),⁵ with which one is able to extract, if not the *phase* of the superconducting order-parameter (OP), then at least the \mathbf{k} -dependence of its modulus at various temperatures and chemical compositions. Here, \mathbf{k} is a wave-vector ranging over the first Brillouin zone (1BZ) of the appropriate inverse lattice for the cuprate compound under consideration. In particular, there is a growing consensus on the occurrence of nodes of the OP along the $k_x = k_y$ direction in the 1BZ

for optimally doped $\text{Bi}_2\text{Sr}_2\text{CaCu}_2\text{O}_8$ (Bi2212).⁶ However, some contradictory claims⁷ for different samples seem to support, in a parallel way, the idea that the detailed \mathbf{k} -space shape of the OP could be a material specific property, although the location of the nodal lines may not be.⁸ This is in agreement with the fact that both the critical temperature T_c itself and the maximum gap at $T = 0$ change considerably from one material to another, as well as within a given material class, on varying the doping level.

We will in this paper try to bring out a few peculiar details of some properties of the superconducting state within the interlayer pair-tunneling mechanism (ILPT), which seems to be almost unique to this pairing mechanism. It is at any rate becoming clear that the determination of the location of nodal lines in the superconducting OP, i.e. its transformation properties under the symmetry operations of the underlying lattice, by no means suffices to unambiguously determine the unconventional pairing mechanism. In this sense, the *symmetry* of the OP is perhaps not a central issue, although it certainly has been the focus of much research during the last few years. Moreover, the controversy over the symmetry of the OP has initiated some of the most sophisticated experiments in condensed matter physics to date.^{9–12}

In this paper, we shall mainly consider the issue of gap anisotropy and competition between different symmetry channels in the $2D$ extended Hubbard model, characterized by a realistic band dispersion, including nearest (N) and next-nearest (NN) neighbors hopping within the

CuO planes, and a small-range in-plane potential, allowing for in-site, N and NN neighbors interaction, in the presence of pair tunneling between adjacent layers.

The issue of the competition among symmetries in the gap function arising from the superconducting instability of an extended Hubbard model at a given band filling has previously been considered in the literature,^{13–16} and has been recently addressed with renewed attention from both the theoretical and experimental points of view, in connection with the Cooper pair instability problem in lattice fermion systems,¹⁷ and with the issue of material specific phenomenology in the cuprates,⁸ respectively.

The ILPT mechanism of high- T_c superconductivity has been proposed as a possible natural explanation for the observed high values of T_c in layered cuprates, as well as a number of other more difficult but related aspects of their complex phenomenology.^{18–20} On the other hand, neither the microscopic origin of the in-plane pairing nor the nature of the pairs has to be specified. Several unconventional properties of these materials, due to strong correlations already in the normal state, support the idea of a breakdown of Fermi liquid theory. In particular, the absence of a Drude peak in the low frequency normal state c -axis optical conductivity, as observed in YBCO²¹ and LSCO,²² would rule out metallic transport along the c -axis in the cuprates. As a consequence, it has been suggested that *coherent* single-particle interlayer tunneling is suppressed, due to the Anderson orthogonality catastrophe,^{19,23,24} whereas coherent pair tunneling in the superconducting phase is not restricted.

Among the mechanisms which would prevent single-particle tunneling, spin-charge separation²⁵ has been proposed. The tunneling process of one fermion would in fact require hopping of both spin and charge degrees of freedom, whereas a singlet object, like a Cooper pair, would carry charge $2e$ but no spin.

Therefore, coherent pair tunneling does not suffer from such restrictions, and enters the total Hamiltonian as a second order effect in the single particle hopping matrix element, $t_{\perp}(\mathbf{k})$, whose dependence on the in-plane wave-vector \mathbf{k} (see Ref. 19 and Eq. (7) below) has recently been confirmed by detailed band structure calculations.²⁶ The main aspect of the ILPT mechanism is that Josephson tunneling of Cooper pairs between adjacent CuO layers dramatically amplifies the superconducting pairing within each layer, by accessing the normal-state frustrated c -axis kinetic energy.

The addition of such a term to the total Hamiltonian does not only greatly enhance T_c , but has also been able to describe the observed absence of the Hebel-Slichter coherence peak in NMR relaxation rate,²⁷ as well as the recent neutron scattering experiments in optimally doped YBCO.²⁸ It was also recognized some time ago^{29–31} that, in the same way as the ILPT mechanism very efficiently boosts the magnitude of T_c arising from the incipient pairing within the planes, essentially due to its near \mathbf{k} -space diagonality, the amplitude as well as the maximum value of the gap function are also dominated by the effec-

tive coupling induced by the ILPT mechanism. *Its actual transformation properties under the symmetry operations of C_{4v} are however governed exclusively by the intralayer contribution to the pairing kernel.*

In this paper, we shall make the latter statement more quantitative, showing how the interlayer coupling determines the detailed \mathbf{k} -dependence of the gap, and actually tends to stabilize one symmetry channel compared to other possible ones, as the chemical potential is varied within the band.

This paper is organized as follows. In Section II we introduce our model and review the basic formalism employed to derive the gap equations. In Section III we discuss the nontrivial numerical problems arising from the solution of the latter equations, due to the presence of the \mathbf{k} -diagonal effective interlayer interaction. A full discussion of the gap symmetry structure, its inherent anisotropy, its maximum values and locations thereof will be included. Calculations of the superconducting density of states (DOS) reveal remarkable structures, due to the gap anisotropy, which are believed to be relevant to the observed anomalous phenomenology in tunneling junction characteristics.³² In Section IV we shall address the issue of determining the critical temperature, as well as the temperature at which symmetry mixing occurs, as a function of the chemical potential. At exactly $T = T_c$ the full \mathbf{k} -dependence of the gap function will be derived analytically, together with the critical exponents of the OP. The resulting expression for the gap function in a closed form will serve as an evidence for the non-trivial anisotropic character and for the symmetry properties of the OP already at the critical point. In Section V we shall consider various thermodynamical quantities in the superconducting phase. Particular attention will be devoted to the normalized jump in the specific heat at the critical point, which, at variance with the BCS conventional result, turns out to be a nonuniversal number, due to symmetry competition and to the ILPT mechanism. In Section VI we summarize our results and present our conclusions.

II. THE MODEL

A. Hamiltonian

The model Hamiltonian we are going to consider in the following describes tightly bound interacting fermions in a bilayer complex:

$$H = \sum_{\mathbf{k}\sigma i} \xi_{\mathbf{k}}^i c_{\mathbf{k}\sigma}^{i\dagger} c_{\mathbf{k}\sigma}^i + \sum_{\mathbf{kk}'ij} \tilde{V}_{\mathbf{kk}'}^{ij} c_{\mathbf{k}\uparrow}^{i\dagger} c_{-\mathbf{k}\downarrow}^{j\dagger} c_{-\mathbf{k}'\downarrow}^j c_{\mathbf{k}'\uparrow}^i, \quad (1)$$

where $c_{\mathbf{k}\sigma}^{i\dagger}$ ($c_{\mathbf{k}\sigma}^i$) creates (destroys) a fermion on the layer i ($i = 1, 2$), with spin projection σ along a specified direction, wave-vector \mathbf{k} belonging to the first Brillouin zone (1BZ) of a 2D square lattice, and band dispersion

$\xi_{\mathbf{k}}^i = \varepsilon_{\mathbf{k}}^i - \mu$, measured relative to the chemical potential μ . The second term in Eq. (1) describes an effective pair interaction, already restricted to the spin singlet channel only, with

$$\tilde{V}_{\mathbf{kk}'}^{ij} = \frac{1}{N} U_{\mathbf{kk}'} \delta_{ij} - T_J(\mathbf{k}) \delta_{\mathbf{kk}'} (1 - \delta_{ij}), \quad (2)$$

where N is the number of sites in the square lattice, $U_{\mathbf{kk}'}$ measures the coupling interaction within each plane, and $T_J(\mathbf{k})$ is the tunneling matrix element between adjacent layers, motivated by Chakravarty *et al.*¹⁹ Equation (2) shows, in particular, how the tunneling mechanism can be equivalently described by an interlayer effective interaction term, although *local* in \mathbf{k} -space.

The main feature of this model is unusual. Although it can be cast in the form of a standard BCS-like effective Hamiltonian, the second term in the pairing potential arises from frustrated kinetic energy along the *c*-axis of the cuprates, unaccessed in the normal state of the high- T_c cuprates. However, it is *lowered* on going into the superconducting state. This is a situation which has no counterpart in conventional Fermi-liquid based superconductors, where the kinetic energy is *enhanced* upon going into the superconducting state, while being overcompensated by a reduction in potential energy. In the above model superconductivity arises via a diametrically opposite mechanism: Instead of having the gain in potential energy overcome the loss of kinetic energy, it is the gain in kinetic energy that is the driving mechanism. There is ample experimental evidence that the kinetic energy is lowered in the superconducting state of the cuprates. Although a confusing point has been that extracted values of the *c*-axis penetration length has been consistent with estimates of Anderson based on gain in kinetic energy,³³ they have also been consistent with *c*-axis conductivity sum rule arguments *ignoring* the gain in kinetic energy. This is traceable to subtleties in applications of *c*-axis conductivity sum rules in unconventional metals, and a nice discussion clearing up this crucial point has recently been presented by Chakravarty.³⁴

Comparison of band structure calculations³⁵ with ARPES results⁵ for various cuprates suggest that the main hybridized single particle band crossing the Fermi level can be correctly described in the case of perfectly isotropic crystal symmetry by the tight-binding dispersion relation (a being the lattice step)

$$\varepsilon_{\mathbf{k}} = -2t[\cos(k_x a) + \cos(k_y a)] + 4t' \cos(k_x a) \cos(k_y a), \quad (3)$$

where it has been recognized³⁶ that at least nearest-neighbors ($t > 0$) as well as next-nearest neighbors ($t' > 0$) hoppings have to be retained, in order to reproduce the most relevant properties common to the mainly 2D band structure of the majority of the cuprate compounds. First and foremost, we have in mind the *shape* of the Fermi surface, but also such features as the Van Hove singularity in the density of states (DOS),

$$n(\mu) = \frac{1}{2N} \sum_{\mathbf{k}} \delta(\varepsilon_{\mathbf{k}} - \mu) \quad (4)$$

at $\mu_{\text{VH}} = -4t'$, shifted towards the band bottom with respect to the mid-band. We hasten to add that we are *not* in any way implying that the Van Hove singularities in the single-particle density of states are important features in explaining the large critical temperatures in these compounds.^{19,20,37} General, and it seems to us very robust arguments for why the Van Hove scenario is not viable, has been given by Anderson.²⁰ These considerations restrict $t'/t \lesssim 0.5$, and imply a flat minimum at the Γ point, which gives rise to a pronounced, though finite, peak in the DOS at the band bottom. This band has a single-particle DOS which can be cast in closed form as^{17,38}

$$n(\varepsilon) = \frac{1}{2\pi^2 t} \frac{1}{\sqrt{1 - b\tilde{\omega}}} \mathbf{K}\left(\sqrt{\frac{1 - [(b + \tilde{\omega})/2]^2}{1 - b\tilde{\omega}}}\right), \quad (5)$$

for $|(\tilde{\omega} + b)/2| < 1$, and zero elsewhere. In Eq. (5) we have defined $b = -2t'/t$, $\tilde{\omega} = \varepsilon/(2t)$, and $\mathbf{K}(\alpha)$ is a complete elliptic integral of the first kind, with modulus α .³⁹ The DOS has a logarithmic singularity $n(\varepsilon) = (2\pi^2 t)^{-1} \sqrt{1 - b^2} [\log(8/|(\tilde{\omega} - b)|) + \log(\sqrt{1 - b^2})]$ at $\varepsilon = 2bt$, a finite cusp at the lower band-edge $n[\varepsilon = -2t(2 + b)] = [4\pi t(1 + b)]^{-1}$, while the DOS at the upper band-edge is given by $n[\varepsilon = 2t(2 - b)] = [4\pi t(1 - b)]^{-1}$. These features of the DOS are important in stabilizing various symmetry channels of the OP as the doping level is varied.¹⁷ A value of the nearest neighbors hopping parameter ranging around $t = 0.25$ eV satisfactorily models the band structure and the shape of the Fermi surface of the majority of the cuprate compounds.^{40,41} It is not among the main aims of this work to specify the microscopic origin of the in-plane potential $U_{\mathbf{kk}'}$.⁴² However, any potential with the symmetry of the underlying lattice may be expanded as a bilinear combination of basis functions for the irreducible representations of the crystal point group, which is C_{4v} for the 2D square lattice.⁴³ Assuming a finite-ranged potential, a finite subset of all the basis-functions (an infinite orthonormal set) will suffice. Retaining therefore only on-site, nearest and next-nearest neighbors in-plane interactions, and projecting out interaction terms in the spin triplet channel, one obtains the following expression for $U_{\mathbf{kk}'}$, which is *separable* in \mathbf{k} -space:

$$U_{\mathbf{kk}'} = \sum_{\eta=0}^4 \lambda_{\eta} g_{\eta}(\mathbf{k}) g_{\eta}(\mathbf{k}'), \quad (6)$$

where $g_0(\mathbf{k}) = 1$, $g_1(\mathbf{k}) = \frac{1}{2}[\cos(k_x a) + \cos(k_y a)]$, $g_2(\mathbf{k}) = \cos(k_x a) \cos(k_y a)$, $g_3(\mathbf{k}) = \frac{1}{2}[\cos(k_x a) - \cos(k_y a)]$, $g_4(\mathbf{k}) = \sin(k_x a) \sin(k_y a)$, and λ_{η} ($\eta = 0, 1, \dots, 4$) are phenomenological effective coupling constants. One immediately recognizes $g_0(\mathbf{k})$, $g_1(\mathbf{k})$, $g_2(\mathbf{k})$ to display (extended) *s*-wave symmetry, whereas $g_3(\mathbf{k})$

and $g_4(\mathbf{k})$ display d -wave symmetry. In the following, we shall assume repulsive on-site and attractive intersite coupling parameters ($\lambda_0 > 0$ and $\lambda_1, \lambda_3 < 0$), choosing their actual values in order to reproduce the correct order of magnitude for the critical temperature and gap maximum at $T = 0$ for the cuprates. Throughout this paper, we keep $\lambda_2 = \lambda_4 = 0$.

Monte Carlo simulations support the idea that short-range antiferromagnetic fluctuations may produce an *attractive* intersite interaction (see Ref. 44 for a review). In our work, however, such an interaction is taken as *phenomenological*, in the sense that an intersite attraction is at least required within an extended Hubbard model if one expects a d -wave contribution to the OP from the lowest lattice harmonics. Remarkably, a perfectly tetragonal lattice requires $\lambda_1 = \lambda_3$. Therefore, if one looks for d -wave coupling, i.e. a contribution from $g_3(\mathbf{k})$ to $U_{\mathbf{kk}'}$, then one should be also prepared to competition with extended s -wave contributions, coming at least from $g_2(\mathbf{k})$.

Finally, we assume the local dependence of the interlayer pair tunneling matrix element as $T_J(\mathbf{k}) = t_\perp^2(\mathbf{k})/t$, i.e. a second-order perturbation in the hopping matrix element $t_\perp(\mathbf{k})$ orthogonal to the CuO layers. Recent detailed band structure calculations²⁶ formally confirm the original choice of functional form made by Chakravarty *et al.*:¹⁹

$$t_\perp(\mathbf{k}) = \frac{t_\perp}{4} [\cos(k_x a) - \cos(k_y a)]^2, \quad (7)$$

which was arrived at by inspection of ARPES data combined with analyticity arguments.

In particular, \mathbf{k} -diagonality expresses conservation of the momentum component \mathbf{k}_\parallel parallel to the CuO₂ plane during the hopping process.

We shall see in the numerical cases below that a fine tuning of t_\perp in the range 0.1—0.15 eV is the main ingredient to reproduce the observed critical temperatures and zero-temperature gap maxima in different compounds. Such a range is however consistent with band structure calculations of t_\perp .²⁶

B. Mean-field treatment

A straightforward mean-field (MF) treatment of the total Hamiltonian Eq. (1) yields the approximate expression:⁴⁵

$$H_{\text{MF}} = \sum_{\mathbf{k}\sigma i} \xi_{\mathbf{k}}^i c_{\mathbf{k}\sigma}^{i\dagger} c_{\mathbf{k}\sigma}^i + \sum_{\mathbf{k}i} [\Delta_{\mathbf{k}}^i c_{\mathbf{k}\uparrow}^{i\dagger} c_{-\mathbf{k}\downarrow}^i + \text{H.c.}], \quad (8)$$

where the auxiliary complex *scalar* field (i.e., the gap function)

$$\begin{aligned} \Delta_{\mathbf{k}}^i &= \sum_{j\mathbf{k}'} \tilde{V}_{\mathbf{k}\mathbf{k}'}^{ij} b_{\mathbf{k}}^j \\ &= \frac{1}{N} \sum_{\mathbf{k}'} U_{\mathbf{k}\mathbf{k}'} b_{\mathbf{k}'}^i - T_J(\mathbf{k}) b_{\mathbf{k}}^j (1 - \delta_{ij}), \end{aligned} \quad (9)$$

has been introduced. The gap function for the i th layer is thus seen to depend on the pair amplitude $b_{\mathbf{k}}^i = \langle c_{-\mathbf{k}\downarrow}^i c_{\mathbf{k}\uparrow}^i \rangle$ in the same layer, through the intralayer potential $\tilde{U}_{\mathbf{k}\mathbf{k}'}$, and on the pair amplitude in the adjacent layer, $b_{\mathbf{k}'}^j$, through the interlayer tunneling amplitude $T_j(\mathbf{k})$, which acts as an effective potential, local in \mathbf{k} -space.

Equation (9) explicitly shows that, in general, the interlayer tunneling mechanism endows the gap function with a nontrivial, nonlocal structure in the direction orthogonal to the CuO layers. Such a dependence is of course relevant in the more general case of multi-layered compounds, and its consequences on T_c have been studied, to some extent, by one of the present authors.²⁹ A generalization of the methods of the present work to multi-layered systems, *below* T_c is straightforward, and is expected to unveil further features in the gap anisotropy, due to the coupling of the gap functions in adjacent layers.

In the case of a simple bilayer ($i = 1, 2$), the simplifying hypothesis that the pair amplitude $b_{\mathbf{k}}^i$ as well as the in-plane single-particle band dispersion $\xi_{\mathbf{k}}^i$ and gap function $\Delta_{\mathbf{k}}^i$ do not depend on the layer index i allows us to decouple the MF Hamiltonian Eq. (8) into a sum of independent Hamiltonians within each layer:¹⁹

$$H_{\text{MF}} = \sum_i \left\{ \sum_{\mathbf{k}\sigma} \xi_{\mathbf{k}} c_{\mathbf{k}\sigma}^{i\dagger} c_{\mathbf{k}\sigma}^i + \sum_{\mathbf{k}} [\Delta_{\mathbf{k}} c_{\mathbf{k}\uparrow}^{i\dagger} c_{-\mathbf{k}\downarrow}^i + \text{H.c.}] \right\}. \quad (10)$$

Standard diagonalization techniques in each layer then yield for $\Delta_{\mathbf{k}}$ the BCS-like gap equation at the finite temperature T :

$$\Delta_{\mathbf{k}} = - \sum_{\mathbf{k}'} \tilde{U}_{\mathbf{k}\mathbf{k}'} \chi_{\mathbf{k}'} \Delta_{\mathbf{k}'}, \quad (11)$$

where $\chi_{\mathbf{k}} = (2E_{\mathbf{k}})^{-1} \tanh(\beta E_{\mathbf{k}}/2)$ denotes the pair susceptibility, $\beta = (k_B T)^{-1}$, and $E_{\mathbf{k}} = \sqrt{\xi_{\mathbf{k}}^2 + |\Delta_{\mathbf{k}}|^2}$ the upper band of the quasiparticle gapped spectrum. In Eq. (11) the pairing potential $\tilde{U}_{\mathbf{k}\mathbf{k}'} = \frac{1}{N} U_{\mathbf{k}\mathbf{k}'} - T_J(\mathbf{k}) \delta_{\mathbf{k}\mathbf{k}'}$ includes the finite-range intralayer as well as the local interlayer effective interactions. More explicitly, Equation (11) reads

$$\Delta_{\mathbf{k}} = - \frac{1}{1 - T_J(\mathbf{k}) \chi_{\mathbf{k}}} \frac{1}{N} \sum_{\mathbf{k}'} U_{\mathbf{k}\mathbf{k}'} \chi_{\mathbf{k}'} \Delta_{\mathbf{k}'}. \quad (12)$$

Making use of Eq. (2) for the intralayer potential allows us to express the gap function as

$$\Delta_{\mathbf{k}} = \frac{1}{1 - T_J(\mathbf{k}) \chi_{\mathbf{k}}} \sum_{\eta} g_{\eta}(\mathbf{k}) \Delta_{\eta}, \quad (13)$$

with

$$\Delta_{\eta} = - \lambda_{\eta} \frac{1}{N} \sum_{\mathbf{k}'} g_{\eta}(\mathbf{k}') \chi_{\mathbf{k}'} \Delta_{\mathbf{k}'}. \quad (14)$$

At a generic temperature T , Equation (13) does not yield immediately the explicit \mathbf{k} -dependence of $\Delta_{\mathbf{k}}$ as it would in the limit of no interlayer tunneling ($T_J \rightarrow 0$). This is due to the unusual prefactor $[1 - T_J(\mathbf{k})\chi_{\mathbf{k}}]^{-1}$, which includes $|\Delta_{\mathbf{k}}|$ self-consistently via the pair susceptibility $\chi_{\mathbf{k}}$. However, this prefactor manifestly displays s -wave symmetry, since $|\Delta_{\mathbf{k}}|$ enters the pair susceptibility $\chi_{\mathbf{k}}$ via the quasiparticle dispersion $E_{\mathbf{k}}$, which is an eigenvalue of H_{MF} , and $T_J(\mathbf{k})$ has s -wave symmetry by itself [Eq. (7)]. Therefore, the complex parameters Δ_{η} , which weigh the basis functions $g_{\eta}(\mathbf{k})$ in Eq. (13), measure the contributions from the different symmetry channels to the full gap function, $\Delta_{\mathbf{k}}$, at a given temperature T . We emphasize that such parameters are *not* order parameters in themselves. Only $\Delta_{\mathbf{k}}$ as a whole serves as an OP for the superconductive instability, whose onset temperature T_c is well defined and unique (see Sec. IV below). However, a vanishing value of some of the Δ_{η} is a signal for the absence of the symmetry contribution which they represent to the full gap function. Besides, the set of parameters $\{\Delta_{\eta}\}$ is not unique. Coefficients of any other complete orthonormal set of functions would also suffice as a basis for expanding the gap function. The above choice of basis functions is convenient, since the expansion of the in-plane pairing kernel used in this paper as bilinear combination of basis functions truncates after just five terms ($\eta = 0, \dots, 4$). However, irrespective of the choice of basis functions made, when all contributions are summed up with appropriate weight-factors, the result *is* unique. Moreover, the use of several parameters Δ_{η} does not attribute to $\Delta_{\mathbf{k}}$ the structure of a multi-component (i.e., vectorial) OP. We reserve the use of multi-component OP to situations encountered in systems such as ^3He and possibly UPt_3 .^{46,47} The OP of high- T_c cuprates is much simpler, with only an amplitude and a phase. On occasions, the set $\{\Delta_{\eta}\}$ is referred to, incorrectly, as the components of a multi-component OP of the cuprates.

We finally remark that the self-consistent expression (13) endows $\Delta_{\mathbf{k}}$ with an inherently anisotropic \mathbf{k} -dependence, which is modulated by the \mathbf{k} -harmonics $g_{\eta}(\mathbf{k})$, displaying explicit symmetry. This is best seen in the limit $T \rightarrow T_c - 0$, where the gap is vanishingly small, so that $\chi_{\mathbf{k}}$ in the right-hand side of Eq. (14) can be approximated by its normal state value, viz. $\chi_{\mathbf{k}}^{0c} = (2\xi_{\mathbf{k}})^{-1} \tanh(\beta_c \xi_{\mathbf{k}}/2)$. Only in such a limit, Equation (14) already yields the explicit expression for the \mathbf{k} -dependence of the gap function, as a product of the anisotropic prefactor $[1 - T_J(\mathbf{k})\chi_{\mathbf{k}}^{0c}]^{-1}$ and a superposition of \mathbf{k} -harmonics, weighted with vanishingly small coefficients Δ_{η} . We shall precise the latter statement in Sec. IV B below, where the full \mathbf{k} -dependence of an incipiently opening gap function at $T = T_c$ will be derived analytically. It will be shown in Sec. IV that at $T = T_c$ the presence of a given symmetry contribution to the (just opening) gap function generally excludes mixing with other symmetries. The latter is possible at lower temperatures, due to the highly nonlinear structure of

the gap equations below the critical temperature, at least within a given range of the band filling. The mutual exclusion of orthogonal symmetries in the gap function at $T = T_c$ is a well-known result in the case of nonlocal, separable potentials.^{48,49} We therefore recover this result also with \mathbf{k} -diagonal contributions to the potential, such as the interlayer pair-tunneling effective interaction.

III. GAP FUNCTION ANISOTROPY AND SYMMETRY

A. The auxiliary gap parameters Δ_{η}

Substituting Δ_{η} from Eq. (14) into Eq. (13) yields

$$\sum_{\eta'} (\delta_{\eta\eta'} + \lambda_{\eta} M_{\eta\eta'}) \Delta_{\eta'} = 0, \quad (15)$$

with

$$M_{\eta\eta'} = \frac{1}{N} \sum_{\mathbf{k}} \tilde{\chi}_{\mathbf{k}} g_{\eta}(\mathbf{k}) g_{\eta'}(\mathbf{k}), \quad (16)$$

where $\tilde{\chi}_{\mathbf{k}} = \chi_{\mathbf{k}}/[1 - T_J(\mathbf{k})\chi_{\mathbf{k}}]$ clearly acquires the role of a ‘renormalized’ pair susceptibility.¹⁹ These equations are in general coupled transcendental equations for $\Delta_{\mathbf{k}}$, and thus define a highly nonlinear problem. Only at $T = T_c$ will the situation simplify considerably, as will be discussed below.

However, once self-consistency has been achieved, Equations (15) are *formally* linear and homogeneous in the *phases* of the complex parameters Δ_{η} , which are responsible for the overall complex phase of $\Delta_{\mathbf{k}}$, as shown by Eq. (13). Due to symmetry considerations, as remarked in Sec. IV A below, Equation (15) reduces to two *formally* independent sets of equations, with real coefficients, one for each group of parameters belonging to either s - or d -wave symmetry. This means that the complex parameters Δ_{η} belonging to the same symmetry are all defined up to a *same common* phase factor. One can therefore speak of a relative phase between s - and d -wave contributions. In particular, it follows that there cannot be anisotropies in \mathbf{k} -space of the *phase* of the order parameter, other than the (trivial) one arising from eventual relative phase differences between two different symmetry contributions. (This justifies the widely used terminology of $s + id$ symmetry, for example.)

Due to the presence of the unusual prefactor $[1 - T_J(\mathbf{k})\chi_{\mathbf{k}}]^{-1}$ in Eq. (13), which itself must be determined self-consistently by finding $\Delta_{\mathbf{k}}$, ordinary numerical procedures used to solve BCS-like gap equations in the presence of separable potentials^{17,14,13,50} are not applicable to the present case. Therefore, remarkably, the gap parameters Δ_{η} are not enough to define the gap function completely: They yield information only about its overall symmetry, on the degree of admixture of the various

symmetry channels in the gap function, and on their relative phase. The solution for $\Delta_{\mathbf{k}}$, therefore, has to be obtained iteratively for each wave-vector \mathbf{k} of interest. The iterative numerical procedure employed to solve the gap equations is briefly outlined in App. A.

We can now proceed with the solution of the gap equation for each given value of the chemical potential μ and temperature T . We first keep μ at a fixed value. By slowly decreasing the temperature from a relatively high value, we observe the appearance of a nontrivial solution to the gap equations, $\Delta_{\mathbf{k}}$, at a critical temperature $T_c = T_c(\mu)$, whose value has been made comparable to the critical temperatures observed in the cuprates, by a suitable tuning of parameters. This onset is signalled by a nonvanishing value of *some* of the parameters Δ_{η} , corresponding to a nonzero contribution of *one* symmetry channel (Fig. 1). We shall later show that only one orthogonal channel (restricting ourselves in this work either to *s*- or to *d*-wave) can contribute to $\Delta_{\mathbf{k}}$ at $T = T_c$ (see Sec. IV and Ref. 48). Upon further decreasing T below T_c , $|\Delta_{\eta}(T)|$ increases (Fig. 1). Together with $|\Delta_{\eta}|$, we plot in Fig. 1 the maximum value of the gap function over the 1BZ,

$$\Delta_M(\mu; T) = \max_{\mathbf{k}} |\Delta_{\mathbf{k}}(\mu; T)|. \quad (17)$$

One immediately recognizes that Δ_M is considerably enhanced with respect to $|\Delta_{\eta}|$, which are representative of the values it would have had, in the absence of ILPT.

We shall later show analytically (see Sec. IV B below) that Δ_{η} and Δ_M behave like $\sim (T_c - T)^{1/2}$ at $T = T_c - 0$, as it is expected in any mean-field theory for an OP. However, Figure 1 shows that the behavior of some Δ_{η} as functions of T may soon depart from its critical limit close to T_c , depending on the value of the chemical potential. This is to be contrasted with the dependence on temperature of Δ_M , which closely resembles the conventional one in BCS theory. The unconventional temperature dependence of the parameters Δ_{η} below T_c directly stems from their definition, Eq. (14). A different choice of parameters $\{\Delta_{\eta}\}$ would in general lead to a different temperature dependence, except their critical behavior at T_c . On the contrary, we expect the result obtained for Δ_M to be unique, as its value depends more on the ILPT amplitude than on the parametrization employed for the symmetry character of the OP.

Depending on the value of μ , other symmetry channels may begin contributing to the full order parameter $\Delta_{\mathbf{k}}$ as T decreases. This is signalled by a nonzero value of the remaining parameters Δ_{η} , and by an enhancement of the parameters Δ_{η} corresponding to the symmetry channel already active, as in the numerical example shown in Fig. 1. The critical exponent with which the new Δ_{η} 's open at the critical temperature is again $1/2$, as can be shown analytically⁵¹. The temperature $T_m = T_m(\mu)$ at which this happens does *not* correspond to any new instability: The system is already a superconductor, with massive gauge-fluctuations and a finite superconducting

coherence length. No remarkable feature is to be observed in Δ_M as a function of T . Its value depends more on the anisotropy induced by the interlayer tunneling mechanism than on the intralayer potential. At the mean-field level, the OP enhances its overall amplitude and its anisotropy character, by allowing pairs to condense in more symmetry channels.

Symmetry mixing is made possible by the nonlinear character of the gap equations themselves, which becomes increasingly more relevant as the temperature decreases towards $T = 0$, given our choice of an extended in-plane real-space pairing potential. Such a possibility has been already studied in detail by Spathis *et al.*,¹⁴ who used a description in terms of a bifurcation of the gap parameters, and by O'Donovan and Carbotte⁵⁰ in the case of an extended Hubbard model without interlayer pair-tunneling. Consistent results have also been obtained by Otnes and one of the present authors¹⁷ for the Cooper problem in presence of an extended intralayer Hubbard potential.

Inclusion of a \mathbf{k} -diagonal interlayer pair-tunneling term in such a model preserves this feature. A novel effect of the interlayer pair-tunneling is that it strongly influences the competition between *s*- and *d*-wave symmetry channels in the OP, enhancing a dominant symmetry channel compared with the subdominant other one. The matrix element $T_J(\mathbf{k})$ generally reduces the region of symmetry mixing in the (μ, T) phase diagram, as will be discussed more in detail in Sec. IV. The reason is that when a gap amplitude starts to grow at $T = T_c$, the dominant channel will initially suppress pairing in other channels. This is generic to any superconductor allowing mixed symmetries to appear in the OP, also conventional ones. Furthermore, it is important to note that the gap at a certain \mathbf{k} -point in the BZ depends on the gap at all other \mathbf{k} -points via the nonlocality of the intralayer part of the pairing kernel, even though the inter-layer part is local. The result is a strong enhancement of the gap amplitudes in the dominant channels, which then to an even stronger degree will suppress competing channels. The consequences of a possible symmetry mixing on observables will be analyzed below in Sec. V. We note, however, that due to the specific choice of band structure and intra-plane coupling constants, it is well established that *d*-wave pairing will dominate in the vicinity of half-filling, while *s*-wave pairing wins out for low filling fractions. Hence, in the cuprates, T_J will tend to stabilize *d*-wave pairing compared to competing channels, were *d*-wave pairing to be the dominant intralayer channel.

B. The order parameter $|\Delta_{\mathbf{k}}|$

Primarily, the interlayer tunneling amplitude $T_J(\mathbf{k})$ in Eq. (12) affects the overall anisotropic structure of the gap function, and not its symmetry character. To show this, the dependence of Δ_{η} on T at a given chemical

potential μ does not suffice alone. Therefore, in Fig. 2 we show the overall \mathbf{k} -dependence of $|\Delta_{\mathbf{k}}|$ over the whole 1BZ at $T = 0$, for a fixed value of μ . We choose to plot $|\Delta_{\mathbf{k}}|$ along the family of mutually orthogonal lines defined by $\varepsilon_{\mathbf{k}} = \text{const}$ and $\gamma_{\mathbf{k}} = \text{const}$, where $\gamma_{\mathbf{k}}$ is a harmonic conjugate of $\varepsilon_{\mathbf{k}}$. Such a choice is best suited to exhibit and highlight the structure of maxima in the gap function along $\xi_{\mathbf{k}} = 0$.

From the numerical analysis, one clearly observes a nodal line along the $k_x = k_y$ direction for $T_m < T < T_c$, which evolves into a line of local minima as symmetries mix below T_m down to $T = 0$. Moreover, what is more apparent is the presence of rather pronounced lines of maxima whose location in the 1BZ follow the locus of the dispersionless wave-vectors for the normal state quasiparticles, i.e. the would-be Fermi line, defined by $\xi_{\mathbf{k}} = 0$. Absolute maxima (sharp peaks) are located at the intersection of the $\xi_{\mathbf{k}} = 0$ locus with $k_y = 0$ for $\mu < \mu_{\text{VH}}$ (corresponding to a Fermi line closed around the Γ point), or with $k_x = \pi/a$ for $\mu > \mu_{\text{VH}}$ (corresponding to a Fermi line closed around $M = (\pi/a, \pi/a)$). Such features are of course produced by the enhancing prefactor $[1 - T_J(\mathbf{k})\chi_{\mathbf{k}}]^{-1}$ in Eq. (12), which gives its maximum contribution where $T_J(\mathbf{k})\chi_{\mathbf{k}} \approx 1$, i.e. exactly as quoted above.⁵² The reason for the *sharpness* of these features is the \mathbf{k} -diagonality of the inter-layer pair-tunneling term. Similar spikes are difficult to obtain with more conventional, i.e. \mathbf{k} -nondiagonal, contributions to the pairing kernel;⁵³ in such cases we do not get the unusual enhancement factor $[1 - T_J(\mathbf{k})\chi_{\mathbf{k}}]^{-1}$ in the effective pairing susceptibility responsible for the peaks, and anisotropies in the pairing kernel tend to be smeared by integrations. We suggest that improved energy resolution in ARPES is a useful tool to look for sharp features in the gap on the Fermi surface, which appears to be a hallmark of the ILPT mechanism.

The maxima distribution and values of $\Delta_{\mathbf{k}}$ along the Fermi line is in qualitative and quantitative agreement with high-resolution photoemission data available for the bilayer Bi2212.⁶ It is gratifying to recover such results, without making detailed reference to the bilayer band structure.⁵⁴ It requires invoking the ILTP mechanism, where the amplitude $T_J(\mathbf{k})$ depends on \mathbf{k} through Eq. (7) (Ref. 19) in a way which is confirmed by band structure calculations.²⁶

Together with a remarkable \mathbf{k} -dependence of the order parameter, one observes a different temperature variation of $\Delta_{\mathbf{k}}$ depending on the location of \mathbf{k} in the 1BZ, and particularly along the Fermi line $\xi_{\mathbf{k}} = 0$, where anisotropy is enhanced. This is in qualitative agreement with recent ARPES measurements of $\Delta_{\mathbf{k}}$ in underdoped Bi2212 at different points of the Fermi line.⁵⁵

C. Superconducting DOS

One consequence of such a peculiar anisotropy is e.g. given by the superconductive density of states at $T = 0$,

$$n_S(\omega) = \frac{1}{N} \sum_{\mathbf{k}} [u_{\mathbf{k}}^2 \delta(\omega - E_{\mathbf{k}}) + v_{\mathbf{k}}^2 \delta(\omega + E_{\mathbf{k}})], \quad (18)$$

where

$$u_{\mathbf{k}}^2 = \frac{1}{2} \left(1 + \frac{\xi_{\mathbf{k}}}{E_{\mathbf{k}}} \right), \quad (19a)$$

$$v_{\mathbf{k}}^2 = \frac{1}{2} \left(1 - \frac{\xi_{\mathbf{k}}}{E_{\mathbf{k}}} \right) \quad (19b)$$

are the usual expressions for the coherence factors in BCS-like theories,⁵⁶ which hold for an interacting Fermi liquid, in the absence of spectral anomalies.³¹ Equation (18) obviously reduces to $n(\omega)$, Eq. (4), in the limit $\Delta_{\mathbf{k}} \rightarrow 0$. In Fig. 3, we plot the superconducting DOS $n_S(\omega)$ corresponding to a superconducting spectrum $E_{\mathbf{k}}$ with fully anisotropic, prevalently *d*-wave gap function $\Delta_{\mathbf{k}}$, obtained self-consistently at $T = 0$, and the analogous quantity $n_S^d(\omega)$, where a pure *d*-wave gap function $\Delta_{\mathbf{k}}^d = \Delta^d g_3(\mathbf{k})$ has been used, with $\Delta^d = \max_{\mathbf{k}} |\Delta_{\mathbf{k}}|$.

In both cases, a gap opens in the SC spectrum at $\omega = 0$ (i.e., around the Fermi level). However, the minimum at $\omega = 0$ in $n_S^d(\omega)$ is flatter than in $n_S(\omega)$, and the features around $\omega = 0$ are quite less pronounced and less asymmetric with respect to the Fermi level. Such behavior in the superconducting DOS is peculiar to the inter-layer tunneling mechanism, and is promising³² in order to explain the anomalous features observed in tunneling junctions experiments with Bi2212.⁵⁷

To complete our picture of the competition of gap symmetries and anisotropy in the ILPT mechanism, we evaluated $\Delta_{\mathbf{k}}$ at $T = 0$ for chemical potential μ ranging from the bottom to the top of the band. In Fig. 4, we plot $|\Delta_{\eta}(\mu; T = 0)|$ against μ . One observes that *s*-wave symmetry prevails at low band filling, and *d*-wave symmetry at higher filling, which is consistent with earlier results.^{14,13,50,17} In a rather narrow region, an OP with mixed symmetry occurs. Numerical analysis revealed that the ILPT mechanism reduces the extension of the latter with respect to the limit $T_J \rightarrow 0$, thus showing that a local non-separable contribution to the pairing potential frustrates, in general, the coexistence of orthogonal symmetries at low temperatures. We argue, therefore, that a true, generally non-separable potential, of which Eq. (6) is only a truncated expansion over a reduced set of basis functions, could even suppress symmetry mixing entirely. We have however no formal proof of a such a statement, at present.

From a numerical analysis of the gap maximum at $T = 0$, $\Delta_M^0(\mu) = \Delta_M(\mu, T = 0)$ [Eq. (17)], as a function of μ (Fig. 4), we moreover conclude that the ILPT mechanism yields reasonably large values of the gap maximum, as observed experimentally in the HTCS,¹⁹ and that the

actual values of the intralayer coupling constants λ_η contribute only in a minor way. Furthermore, Fig. 4 shows that the largest gaps correspond to prevalently d -wave symmetry, and are obtained for $\mu \approx \mu_{\text{VH}}$ (the exact location depending weakly on λ_η), where the enhancement due to $T_J(\mathbf{k})$ is highest, once more showing the relevance of the $2D$ character of the single particle dynamics in the normal state through their dispersion relation, and the importance of the actual value of the next-nearest neighbors hopping amplitude t' in Eq. (3), which fixes the value of μ at which the Fermi line changes its topology.

IV. CRITICAL TEMPERATURE

Among the many experimental facts concerning the HTCS phenomenology that the ILPT mechanism is able to describe, probably the most apparent is the ease with which the high value of the critical temperature itself is explained. This is first and foremost due to the \mathbf{k} -diagonality of the intralayer part of the kernel, and has previously been investigated in some detail by Chakravarty *et al.*,¹⁹ when considering the ILPT mechanism for bilayer compounds such as Bi2212. Of course, it is a matter of some importance to investigate the effect of inelastic scattering, i.e. \mathbf{k} -space broadening, of the interlayer term, to investigate how detrimental effect it has on T_c . Preliminary results⁵⁸ show that T_c is fairly robust to a broadening of the interlayer term.

In this Section, we generalize the results of Ref. 19 to arbitrary doping, conveniently reparametrized by the chemical potential ranging within the dispersion bandwidth, extending the analysis to the case of the intralayer potential proposed in Eq. (6). The dependence of T_c on μ is a relevant point in itself, since it allows to clarify the role of the $2D$ hole dynamics and that of the incoherent, interlayer pair-tunneling mechanism in determining the shape and extension of the (μ, T) region allowed for the superconductive instability to occur.

A separate question, in the present context, concerns the (μ, T) region allowed to superconductivity characterized by a symmetry order parameter. Due to the structure of the gap equation (12), such a question involves considerable numerical difficulties, in comparison with previous work of some of the present authors,⁵⁹ which will be dealt with in some detail.

A. Superconducting instability: pure symmetry

At $T = T_c$, the mean-field gap function $\Delta_{\mathbf{k}}$ is vanishingly small everywhere in the \mathbf{k} -space. Therefore, Eq. (15) linearizes to

$$\sum_{\eta'} (\delta_{\eta\eta'} + \lambda_\eta M_{\eta\eta'}^0) \Delta_{\eta'} = 0, \quad (20)$$

where the linearized matrix elements

$$\begin{aligned} M_{\eta\eta'}^0 &= \lim_{\Delta_{\mathbf{k}} \rightarrow 0} M_{\eta\eta'} \\ &= \frac{1}{N} \sum_{\mathbf{k}} \frac{\chi_{\mathbf{k}}^0}{1 - T_J(\mathbf{k})\chi_{\mathbf{k}}^0} g_\eta(\mathbf{k})g_{\eta'}(\mathbf{k}) \end{aligned} \quad (21)$$

do not depend on $\Delta_{\mathbf{k}}$ any more. These matrix elements are analogs of the well-known logarithmically divergent integrated pairing susceptibility in the BCS-theory.⁶⁰ Here, what appears are integrated, effective pairing susceptibilities, projected down on various symmetry channels. Symmetry dictates that only basis functions having the same transformation properties, albeit belonging to different irreducible representations of C_{4v} , can yield a finite effective pairing susceptibility $M_{\eta\eta'}^0$.

The condition for Eq. (20) to have a nontrivial solution $\{\Delta_{\eta'}\}$ is that

$$\det(\delta_{\eta\eta'} + \lambda_\eta M_{\eta\eta'}^0) = 0. \quad (22)$$

Due to the s -wave symmetry character of $\tilde{\chi}_{\mathbf{k}}^0$ and the definite symmetry character of the basis functions $g_\eta(\mathbf{k})$, $M_{\eta\eta'}^0$ is block-diagonal. Its elements are nonzero if and only if η and η' denote symmetry channels belonging to the same irreducible representation of the crystal point group. Therefore, Eq. (22) for T_c at a given μ factorizes into

$$D_{\lambda_s}^0(\mu, T) D_{\lambda_d}^0(\mu, T) = 0, \quad T = T_c. \quad (23)$$

Here, $D_{\lambda_h}^0(\mu, T_c) = \det(\delta_{\eta_h\eta'_h} + \lambda_{\eta_h} M_{\eta_h\eta'_h}^0)$ ($h = s, d$) depends only on a subset of the λ_η ($\eta = \eta_h$). Linearization therefore decouples the two symmetries at $T = T_c$. The solution corresponding to the largest value of T_c from Eq. (23) corresponds to the true superconducting transition temperature. The transformation properties of the corresponding eigenvectors determine in which (single) symmetry channel the dominant superconducting instability occurs. At $T = T_c$, the other solution corresponds to a subdominant superconducting instability, and is physically irrelevant. Generically, precisely at $T = T_c$, we thus cannot have an instability into a mixed state, i.e. a superconducting instability with eigenvectors having components belonging to different irreducible representations of C_{4v} . A mixing of symmetries can only occur below the physical T_c , as discussed more in detail in Sec. III. The exception to this statement occurs when μ is fine-tuned such that the zeroes of the d - and s -determinants are found at the same temperature. The phase space for this to occur is however vanishingly small. Such a result is a generalization of a known theorem, which applies to purely nonlocal separable extended potentials.^{48,49} The generalization has been made possible by the definite symmetry character (s -wave) of the effective local potential induced by the interlayer tunneling amplitude $T_J(\mathbf{k})$ in Eq. (2), and is of course extendible to potentials supporting an arbitrary number of symmetry channels in the OP.⁶¹ We emphasize that these statements pertain to

the square lattice only. In systems with pronounced *ab*-plane orthorhombicity, such as YBCO, a certain amount of mixing is expected on quite general grounds, and is indeed inevitable. The underlying lattice point group is C_{2v} , and thus an expansion in terms of basis functions for C_{4v} will yield several terms.

The issue of determining $T_c = T_c(\mu)$ and the symmetry channel in which the instability occurs, proves therefore to be equivalent to comparing the two solutions of Eq. (23). It must be noted, however, that at variance with the case of no interlayer tunneling, the linearized matrix elements $M_{\eta\eta'}^0$ included in the definitions of $D_{\lambda_h}^0(\mu, T_c)$ display a divergent behavior at some value $T_c = T^*(\mu)$, due to the presence of the denominator $1 - T_J(\mathbf{k})\chi_{\mathbf{k}}^0$ in the summand of Eq. (21). It has already been emphasized⁵² that the self-consistency condition Eq. (12) for a nonvanishing gap $\Delta_{\mathbf{k}}$ below the true T_c prevents the occurrence of such a singularity. The singularity is due only to the mathematical artifact of extending the definitions of the determinants $D_{\lambda_h}^0(\mu, T_c)$ to a domain below their zeroes. This is not physically meaningful, since the opening of $\Delta_{\mathbf{k}}$ modifies their very definitions.

The occurrence of such an unusual singularity in the integrated effective pairing-susceptibility, projected on various symmetry channels, has a physical meaning. It shows how the action of an interlayer pair-tunneling mechanism bounds the critical temperature from below, and therefore enhances it. Given an intraplane contribution to the pairing-kernel, a lower bound on T_c is set by the matrix element T_J ; the lower bound roughly given by $T_J/4$ (see Eq. (24) below). Beyond this, the actual value of T_c is fixed by the intralayer coupling symmetry and strength. As already noted, $\chi_{\mathbf{k}}^0$ is maximum along the Fermi line, where $\lim_{T \rightarrow T_c} \lim_{\xi_{\mathbf{k}} \rightarrow 0} \chi_{\mathbf{k}}^0 = \beta_c/4$. Therefore, the renormalized susceptibility $\tilde{\chi}_{\mathbf{k}}^0$ along the Fermi line is maximum where $T_J(\mathbf{k})$ is maximum, i.e. at the intersection of the Fermi line with the Γ -X-M path in the 1BZ (and symmetry related points). Looking for the highest temperature $T^*(\mu)$ at which the maximum of $\tilde{\chi}_{\mathbf{k}}^0$ diverges, one has therefore to distinguish between the two possible topologies for the Fermi line arising from Eq. (3). One finds, analytically,

$$k_B T^*(\mu) = \begin{cases} \frac{T_J}{64} \left(\frac{\mu_{\perp} - \mu}{\mu_{\perp} + 2t} \right)^4, & \mu_{\perp} \leq \mu < \mu_{\text{VH}}, \\ \frac{T_J}{64} \left(\frac{\mu_{\top} - \mu}{\mu_{\top} + 2t} \right)^4, & \mu_{\text{VH}} \leq \mu \leq \mu_{\top}, \end{cases} \quad (24)$$

where μ_{\perp}, μ_{\top} denote the bottom and the top of the band, respectively, which generalizes the expression given in Ref. 19. At the Van Hove singularity, $T^*(\mu)$ is maximum, with $k_B T^*(\mu_{\text{VH}}) = T_J/4 = t_{\perp}^2/4t$, yielding a lower bound $k_B T_c \lesssim 0.01$ eV ($T_c \lesssim 110$ K), which is a representative value for most bilayer cuprates.

Figure 5 shows our results for T^* and T_c as functions of μ . The values of the parameters have been chosen as quoted in order to yield a critical temperature at optimal doping whose value is representative of the bilayer

cuprate superconductors. Superconductivity appears restricted predominantly to the lower part of the band, even though a nonvanishing lower bound $T^*(\mu)$ assures a nonzero, albeit decreasing, T_c , as μ increases towards the top of the band. In that regime, however, we showed numerically that Δ_M^0 is vanishingly small (cf. Fig. 4). As previously observed,^{59,17} *s*-wave symmetry prevails near the bottom of the band, whereas *d*-wave symmetry wins out as μ increases. A robust qualitative argument for this was given in Ref. 17. The critical temperature T_c reaches its optimal value near $\mu = \mu_{\text{VH}}$, the exact location depending on the set of values $\{\lambda_{\eta}\}$ actually chosen for the intralayer coupling parameters.

B. Gap anisotropy at the critical point

The ILPT mechanism is seen to strongly enhance the \mathbf{k} -space anisotropy of the gap function also at $T = T_c$, regardless of the symmetry character that the OP takes on, which at the critical point is unambiguously defined (no mixing). This is already apparent from Eq. (13), and can be proved by exhibiting the full analytical \mathbf{k} -dependence of the gap function $\Delta_{\mathbf{k}}$, at $T = T_c - 0$.

For $T \lesssim T_c$, one may Taylor expand all quantities of interest in powers of $\beta^2 |\Delta_{\mathbf{k}}|^2 \ll 1$, safely retaining the first nonzero term only. From Eq. (16), one obtains:

$$M_{\eta\eta'} = M_{\eta\eta'}^0 - \beta^3 \frac{1}{N} \sum_{\mathbf{k}} \frac{\phi(\beta\xi_{\mathbf{k}}/2)}{[1 - T_J(\mathbf{k})\chi_{\mathbf{k}}^0]^2} g_{\eta}(\mathbf{k}) g_{\eta'}(\mathbf{k}) |\Delta_{\mathbf{k}}|^2 + \mathcal{O}(\beta^2 |\Delta_{\mathbf{k}}|^2), \quad (25)$$

where

$$\phi(x) = \frac{1}{32x^3} (\tanh x - x \operatorname{sech}^2 x), \quad (26)$$

and a superscript zero denotes that the limit $\Delta_{\mathbf{k}} \rightarrow 0$ has been taken. At $T = T_c$, only one symmetry channel is active, therefore Equation (23) is satisfied by the vanishing of one block determinant, say $D_{\lambda_h}^0(\mu, T_c) = 0$, ($h = s$ or d). Expanding $D_{\lambda_h}(\mu, T)$ around $\beta^2 |\Delta_{\mathbf{k}}|^2 = 0$ and making use of Eq. (25), one finds:

$$D_{\lambda_h}(\mu, T) = D_{\lambda_h}^0(\mu, T) - \beta^3 \frac{1}{N} \sum_{\mathbf{k}} \frac{\phi(\beta\xi_{\mathbf{k}}/2)}{[1 - T_J(\mathbf{k})\chi_{\mathbf{k}}^0]^2} \times \left(\sum_{\eta\eta'}^h \lambda_{\eta} g_{\eta}(\mathbf{k}) W_{\eta\eta'}^0 g_{\eta'}(\mathbf{k}) \right) |\Delta_{\mathbf{k}}|^2 + \mathcal{O}(\beta^2 |\Delta_{\mathbf{k}}|^2), \quad (27)$$

where $W_{\eta\eta'}$ denotes the cofactor for the element $\delta_{\eta\eta'} + \lambda_{\eta} M_{\eta\eta'}$ in D_{λ_h} , and a superscript h restricts the sum to η and η' corresponding to the h -wave channel only. We observe, then, that close to T_c , Equations (20) factorize into two separate, independent sets of linear homogeneous equations for the parameters Δ_{η} representing

either symmetries, respectively. In the proximity of T_c , therefore, since $D_{\lambda_h}^0(\mu, T) = 0$ at $T = T_c(\mu)$, only the set of equations for Δ_η corresponding to the incipient h -wave channel admits a nontrivial solution, readily given by:

$$|\Delta_\eta| = W_{\bar{\eta}\eta}^0 \epsilon, \quad (28)$$

where $\bar{\eta} \in \{0, 1, 2\}$, if $h = s$, or $\bar{\eta} \in \{3, 4\}$, if $h = d$, and ϵ is an homogeneity factor, common for all η 's, which vanishes as $T \rightarrow T_c - 0$, as specified in the following. In deriving Eq. (28), we made use of the fact that, in the absence of symmetry mixing, such as at the critical point, all the Δ_η belonging to a given symmetry channel share the same complex phase factor. Inserting Eq. (13) into Eq. (27), and making use of Eq. (28), one finds:

$$\epsilon^2 = \frac{1}{\beta^3} \frac{D_{\lambda_h}^0(\mu, T)}{C_{\lambda_h}^0(\mu, T)}, \quad (29)$$

where

$$\begin{aligned} C_{\lambda_h}^0(\mu, T) &= \frac{1}{N} \sum_{\mathbf{k}} \frac{\phi(\beta\xi_{\mathbf{k}}/2)}{[1 - T_J(\mathbf{k})\chi_{\mathbf{k}}^{0c}]^4} \\ &\times \left(\sum_{\eta\eta'}^h \lambda_\eta g_\eta(\mathbf{k}) W_{\eta\eta'}^0 g_{\eta'}(\mathbf{k}) \right) \\ &\times \left(\sum_{\eta}^h W_{\bar{\eta}\eta}^0 g_\eta(\mathbf{k}) \right)^2. \end{aligned} \quad (30)$$

We finally observe that, by construction, $\lim_{T \rightarrow T_c} D_{\lambda_h}^0(\mu, T) = 0$. Therefore, the expansion of Eq. (29) around $T = T_c$ begins from the linear term in $(T - T_c)$, and one straightforwardly obtains:

$$\epsilon = \alpha_h \frac{T_c}{2} \left(1 - \frac{T}{T_c} \right)^{1/2}, \quad (31)$$

where

$$\alpha_h^2 = \frac{1}{C_{\lambda_h}^{0c}} \sum_{\eta\eta'}^h \lambda_\eta H_{\eta\eta'}^{0c} W_{\eta\eta'}^{0c}, \quad (32a)$$

$$H_{\eta\eta'}^0 = \frac{1}{N} \sum_{\mathbf{k}} \frac{g_\eta(\mathbf{k}) g_{\eta'}(\mathbf{k})}{[1 - T_J(\mathbf{k})\chi_{\mathbf{k}}^{0c}]^2} \operatorname{sech}^2 \left(\frac{1}{2} \beta \xi_{\mathbf{k}} \right), \quad (32b)$$

and a superscript c denotes that the limit $T \rightarrow T_c$ has been taken. Making use of Eq. (31) in the expansions for $|\Delta_\eta|$ and $|\Delta_{\mathbf{k}}|$, Eqs. (28) and (13), respectively, at the critical point, one explicitly obtains:

$$|\Delta_\eta| = \alpha_h \frac{T_c}{2} \left(1 - \frac{T}{T_c} \right)^{1/2} W_{\bar{\eta}\eta}^{0c}, \quad (33a)$$

$$|\Delta_{\mathbf{k}}| = \alpha_h \frac{T_c}{2} \left(1 - \frac{T}{T_c} \right)^{1/2} \frac{\sum_{\eta}^h W_{\bar{\eta}\eta}^{0c} g_\eta(\mathbf{k})}{1 - T_J(\mathbf{k})\chi_{\mathbf{k}}^{0c}}. \quad (33b)$$

Equation (33b) *analytically* yields the \mathbf{k} -dependence of the gap function at the critical point. In order to exhibit more clearly the role of the ILPT amplitude $T_J(\mathbf{k})$ in establishing such dependence, one may consider the limiting case in which only one basis function (say, $\eta = \star$) contributes to the expansion of $\Delta_{\mathbf{k}}$. On taking the limit $|\lambda_\star/\lambda_\eta| \rightarrow \infty$, $\forall \eta \neq \star$, one recovers the result (see also Ref. 62):

$$|\Delta_{\mathbf{k}}| = \alpha_\star \frac{T_c}{2} \left(1 - \frac{T}{T_c} \right)^{1/2} \frac{g_\star(\mathbf{k})}{1 - T_J(\mathbf{k})\chi_{\mathbf{k}}^{0c}}, \quad (34)$$

where

$$\alpha_\star^2 = \frac{\frac{1}{N} \sum_{\mathbf{k}} \frac{g_\star^2(\mathbf{k})}{[1 - T_J(\mathbf{k})\chi_{\mathbf{k}}^{0c}]^2} \operatorname{sech}^2 \left(\frac{1}{2} \beta c \xi_{\mathbf{k}} \right)}{\frac{1}{N} \sum_{\mathbf{k}} \frac{g_\star^4(\mathbf{k})}{[1 - T_J(\mathbf{k})\chi_{\mathbf{k}}^{0c}]^4} \phi \left(\frac{1}{2} \beta c \xi_{\mathbf{k}} \right)}. \quad (35)$$

From Eqs. (33), one also recovers the critical exponent $1/2$ analytically, which is typical for an order parameter at the critical point, within a mean-field theory. Moreover, Equation (33b) clearly shows that no symmetry mixing is allowed at $T = T_c$, by explicitly exhibiting which basis functions $g_\eta(\mathbf{k})$ contribute to $\Delta_{\mathbf{k}}$, and their weights. The role of the ILPT mechanism is furthermore made evident by the presence of the factor $[1 - T_J(\mathbf{k})\chi_{\mathbf{k}}^{0c}]^{-1}$ in Eq. (33b). This provides the gap function $\Delta_{\mathbf{k}}$ with a remarkable anisotropy already at $T = T_c$, thus showing that such an anisotropy is neither due to self-consistency (at $T = T_c$, the values of $\Delta_{\mathbf{k}}$ at different points in the BZ are independent of each other), nor to nonlinearity (at $T = T_c$, the gap equations can be linearized). On the contrary, gap anisotropy is robust against both self-consistency and nonlinearity, whose relevance increases as T decreases, as our numerical study below T_c has demonstrated.

From Eq. (33b) one is able to predict a line of relative maxima for $|\Delta_{\mathbf{k}}|$ along the $\xi_{\mathbf{k}} = 0$ locus already at $T = T_c$. Absolute maxima occur at the intersection of the $\xi_{\mathbf{k}} = 0$ locus with the Γ - X - M path, and symmetry related points. The sharpness of the maxima is guaranteed by $T_J(\mathbf{k})$, and is therefore distinctive of the ILPT mechanism. Away from $\xi_{\mathbf{k}} = 0$, the gap function is *rapidly* vanishing over the rest of the 1BZ, as an effect of the renormalization of the pair susceptibility, induced by the ILPT mechanism. Moreover, moving along the $\xi_{\mathbf{k}} = 0$ line in \mathbf{k} -space, the gap function $|\Delta_{\mathbf{k}}|$ is seen to decrease *more than linearly* as one approaches $k_x = k_y$, where $|\Delta_{\mathbf{k}}|$ attains a minimum value, which is finite and very small, in the s -wave case, or zero, in the d -wave case. This has to be contrasted with the case of a conventional d -wave gap, $\Delta_{\mathbf{k}} \propto g_3(\mathbf{k})$. In such a limit (corresponding to $T_J \rightarrow 0$ in our model), $\Delta_{\mathbf{k}}$ would vanish *linearly* as \mathbf{k} approaches perpendicularly the nodal line, $k_x = k_y$. A flat minimum (node line) along $k_x = k_y$ is indeed strongly suggested by ARPES results for Bi2212 single crystals,⁵

and has been earlier proposed as a “smoking gun” for the ILPT mechanism by Anderson.⁶³

The sharp anisotropic features of $|\Delta_{\mathbf{k}}|$ are robust against non-linearity, whose relevance increases as T decreases, as shown by Eqs. (13) and (14). Correspondingly, the normal state spectrum at $T = T_c$ gets gapped where $|\Delta_{\mathbf{k}}|$ is maximum *far more significantly* than elsewhere. As T decreases, one can think of the the Fermi line as remaining practically ungapped along disconnected arcs of ever smaller length. These arcs shrink and eventually collapse into a single point along line, as $T \rightarrow 0$.

Recent ARPES experiments in underdoped Bi2212 single crystals by Norman *et al.*⁶⁴ are suggestive of such a scenario. A progressive ‘erosion’ of the Fermi line as temperature decreases has been related to the opening of an unconventional pseudogap, precursor of the superconducting gap which opens at T_c .

V. APPLICATIONS

In mean-field theory, the superconducting paired state is microscopically fully characterized by the gap function $\Delta_{\mathbf{k}}$, which we now have access to over the whole 1BZ as a function of band filling and temperature. In this section, we will discuss how the solution to the gap equations can be employed in the calculation of some specific thermodynamic properties of the system. A number of physical quantities of interest have previously successfully been considered with various such solutions, such as for instance the anomalously large gap anisotropy observed in Bi2212,¹⁹ the non-conventional features in the NMR relaxation rate $1/T_1$ observed in YBCO,²⁷ the variation of T_c with the number of layers,²⁹ the unusual features in the neutron scattering rates observed in YBCO,²⁸ and a possible explanation of the spin-gap, or pseudo-gap.⁶⁵ All of the above quoted calculations utilize the special features of the gap that arise as a consequence of the interlayer pair-tunneling mechanism. In particular, the calculations of the gap anisotropy, the variation of T_c with the size of the unit cell, the neutron scattering peak, and the spin-gap utilize the unique and sharp \mathbf{k} -space features that arise in the solution to the gap equations due to the unusual renormalization of the pairing susceptibility, $\chi_{\mathbf{k}} \rightarrow \chi_{\mathbf{k}}/[1 - T_J(\mathbf{k})\chi_{\mathbf{k}}]$.

We choose to consider quantities that have the promise of being sensitive to the \mathbf{k} -space features of the gap, which are relatively readily obtained, and which are possible to confront straightforwardly with experiments. In the following, we shall mainly focus on the specific heat anomalies of the model, although work is currently in progress concerning the in-plane coherence length and the thermal conductivity.³² These quantities are either sensitive to the presence of the particular T_J -term in the Hamiltonian such as specific heat anomalies, or involve the derivative of the gap such as the coherence length

and the thermal conductivity. Moreover we choose, for application to the high- T_c compounds, parameters such that the critical temperature at optimum doping is given by $T_c = 90$ K.

Although several of the properties of the superconducting state in the high- T_c compounds which in one way or another probe the \mathbf{k} -space structure of the gap are unusual, the thermodynamics seems to be remarkably similar to ordinary superconductors. This is true for instance for the entropy of the system. Is a gap arising from an unconventional gap equation like the one considered in this paper, giving rise to unusual \mathbf{k} -space features in $\Delta_{\mathbf{k}}$, consistent with standard thermodynamic results otherwise normally associated with conventional superconductors?⁶⁶ Although not shown here, we have calculated these quantitites and found that they are remarkably similar to those found in any conventional superconductor.⁶⁶ This is basically because quantities like entropy involve a \mathbf{k} -space integration over smooth functions of the gap. The detailed \mathbf{k} -space features are then washed out and the results are to some extent quite insensitive to these features in $\Delta_{\mathbf{k}}$. The same also pertains to some extent to quantities like the NMR relaxation rate $1/T_1$, which exhibits features in its T -dependence which are reproducible by a gap with a number of different symmetries.^{67,68} This is perhaps not surprising, as this quantity involves a double integration over \mathbf{k} -space vectors. Another matter altogether is the situation where we consider quantities involving only one \mathbf{k} -space integration, and in addition also \mathbf{k} -derivatives of the gap.³²

A. Specific heat

In this subsection, we will consider the specific heat anomalies of the model. The entropy per particle in the superconducting state is given by⁶⁹

$$S^s(\mu, T) = -2k_B \frac{1}{N} \sum_{\mathbf{k}} [f_{\mathbf{k}} \log f_{\mathbf{k}} + (1 - f_{\mathbf{k}}) \log(1 - f_{\mathbf{k}})], \quad (36)$$

where $f_{\mathbf{k}} = [1 + \exp(\beta E_{\mathbf{k}})]^{-1}$ is the Fermi function evaluated with the superconducting spectrum $E_{\mathbf{k}}$.

Differentiating $S^s(\mu, T)$, Eq. (36), with respect to T one obtains the specific heat⁶⁹

$$\begin{aligned} C_V^s(\mu, T) &= T \frac{\partial S^s}{\partial T} \\ &= \frac{1}{2} k_B \beta^2 \frac{1}{N} \sum_{\mathbf{k}} E_{\mathbf{k}} \left(E_{\mathbf{k}} + \beta \frac{\partial E_{\mathbf{k}}}{\partial \beta} \right) \operatorname{sech}^2 \left(\frac{1}{2} \beta E_{\mathbf{k}} \right). \end{aligned} \quad (37)$$

Whenever $E_{\mathbf{k}}$, i.e. $\Delta_{\mathbf{k}}$, contains discontinuities in its temperature-derivative as a function of T , the specific heat Eq. (37) displays a finite peak. This is typical of the mean-field approximation, as mentioned above. In the presence of a competition between several symmetry channels, several such discontinuities may occur, at

$T = T_c$ and at $T = T_m$. However, we expect the height of the second peak at $T = T_m$ to be exponentially reduced with respect to the peak at $T = T_c$, due to the presence of the hyperbolic secant in Eq. (37).

Making use of the gap equations it is possible to derive a straightforward expression for $E_{\mathbf{k}} \partial E_{\mathbf{k}} / \partial \beta$, valid at all $T \leq T_c$, which turns out to be linear in $\partial |\Delta_{\mathbf{k}}|^2 / \partial \beta$ (cf. also App. B). Such a quantity is numerically accessible, in principle, from the solution to the gap equations. Therefore, Equation (37) directly yields the temperature dependence of C_V^s also below T_c . However, such dependence turns out to be conventional, and will not be shown here (see also Ref. 17).

At exactly $T = T_c$, the knowledge of the \mathbf{k} -dependence of $\Delta_{\mathbf{k}}$ in a closed form allows instead to study analytically the jump in the specific heat, normalized with respect to the specific heat in the normal state, C_V^n , i.e. in the absence of the gap, at the same temperature:

$$\frac{\delta C_V^c}{C_V^{nc}} = \frac{C_V^s(\mu, T_c) - C_V^n(\mu, T_c)}{C_V^n(\mu, T_c)}. \quad (38)$$

Making use of Eq. (33b) corresponding to the opening of a generic h -wave symmetry gap ($h = s, d$), one readily obtains:

$$\begin{aligned} \delta C_V^c &= \frac{1}{16} k_B \alpha_h^2 \frac{1}{N} \sum_{\mathbf{k}} \frac{\left(\sum_{\eta}^h W_{\bar{\eta}\eta}^{0c} g_{\eta}(\mathbf{k}) \right)^2}{[1 - T_J(\mathbf{k}) \chi_{\mathbf{k}}^{0c}]^2} \operatorname{sech}^2 \left(\frac{1}{2} \beta_c \xi_{\mathbf{k}} \right), \\ C_V^{nc} &= 2k_B \frac{1}{N} \sum_{\mathbf{k}} \left(\frac{1}{2} \beta_c \xi_{\mathbf{k}} \right)^2 \operatorname{sech}^2 \left(\frac{1}{2} \beta_c \xi_{\mathbf{k}} \right). \end{aligned}$$

We explicitly observe that *only at $T = T_c$* one is able to include in Eq. (37) for C_V^s the analytical expressions for $\Delta_{\mathbf{k}}$ and its T -derivatives: Numerics are only needed in performing the integrations over the 1BZ where required.⁷⁰ Employing the value of $T_c = T_c(\mu)$ numerically obtained as in Sec. IV A (Fig. 5), we are eventually able to evaluate the normalized jump $\delta C_V^c / C_V^{nc}$ in the specific heat at $T = T_c$, as a function of the chemical potential μ . We display our results in Fig. 6, and compare them with the conventional result $\delta C_V^c / C_V^{nc} = 12/[7\zeta(3)] \simeq 1.42613$, derived within the BCS theory for an s -wave, uniform gap function.^{56,66}

We find a remarkable agreement with the BCS limit over an extended plateau, corresponding to the s -wave region in μ . On the contrary, a considerably lower value is obtained, on the average, in the d -wave region, including optimal doping. On the overall, we are thus able to predict a *nonuniversal* ratio $\delta C_V^s / C_V^{nc}$, to be contrasted with the universal BCS value, valid for Fermi-liquid based superconductors.⁶² This is due to the widely anisotropic \mathbf{k} -dependence of the gap function (also close to the critical point), which is mainly traceable to the renormalization of the pairing susceptibility, and is thus a manifestation of the special nature of the interlayer pair tunneling mechanism.

One slightly unusual feature is the possible appearance of a *second peak* in the specific heat at low temperatures. Such a feature is not found in a superconductor with an order parameter transforming exclusively as a single basis function for an irreducible representation of the crystal point group C_{4v} . The result we find originates from the fact that at low temperatures, new symmetry channels couple in to the superconducting order, as shown in Fig. 1. This leads to a cusp in the specific heat, *but not to any new diverging length in the problem*. This second anomaly in the specific heat therefore *does not represent a new superconducting phase transition*, but merely condensation of Cooper pairs into additional symmetry channels. The true order parameter of the problem, $\Delta_{\mathbf{k}}$, becomes finite once and for all at $T = T_c$, and this point represents the only zero-field phase transition. This appears to be a widely misunderstood point in the literature.⁷¹ As mentioned previously, the parameters Δ_{η} do not represent order parameters for this problem. Note that the second anomaly in the specific heat, at low temperatures, is expected to be well captured by mean-field theory. It is located *outside* the critical region of the normal metal-superconductor transition, while this is not the case for the first anomaly in the specific heat located at $T = T_c$. Therefore, our results for the main anomaly in the specific heat, the prominent step-*discontinuity* at the critical point, should be replaced by a near-logarithmic *singularity* characteristic of the 3DXY-model.⁷² This reflects the fact that for optimally doped and underdoped systems, phase-fluctuations in the problem appears to be strong, such that the true superconducting transition occurs well below the mean-field transition.

Our main conclusion of this subsection is that in slightly overdoped compounds the main normalized specific heat anomaly will be mean-field like, but *nonuniversal* due to the appearance of a renormalized pairing susceptibility $\chi_{\mathbf{k}}/[1 - T_J(\mathbf{k}) \chi_{\mathbf{k}}]$, in contrast to the standard BCS result.

VI. SUMMARY AND CONCLUDING REMARKS

We have addressed the issue of the mixing of symmetry channels in the superconducting order parameter for a bilayer superconductor in the presence of an interlayer pair-tunneling mechanism¹⁹ as a possible framework for understanding numerous unconventional features exhibited by the HTCS compounds. Incipient superconductivity has been generated within each individual CuO₂-layer through a Hubbard-like in-plane potential, including primarily an on-site repulsion and nearest-neighbor interaction, which has been strongly enhanced through the inclusion of the interlayer tunneling amplitude $T_J(\mathbf{k})$, as suggested by ARPES as well as by detailed band structure calculations.

A mean-field treatment in the bilayer case allowed a computation of the \mathbf{k} -dependence of the in-plane order

parameter $\Delta_{\mathbf{k}}$. A suitable numerical procedure has been devised in order to solve the inherently nonlinear gap equations. It has been possible to study the evolution of the symmetry character of the gap function versus temperature and chemical potential, and unveil a competition between *s*-wave and *d*-wave character in $\Delta_{\mathbf{k}}$. In this description, $\Delta_{\mathbf{k}}$ is a *single complex scalar* order parameter. No multi-component OP has to be claimed for, which would imply the existence of ‘more’ condensates with different ‘features,’ as elsewhere reported in the literature.⁴ In particular, no transition of the normal-to-superconductor kind is expected when symmetries are allowed to mix: The system is already a superconductor with an open energy gap, whose structure in \mathbf{k} -space only evolves, thus allowing pairs to condense into more symmetry channels.

Moreover, a surprisingly anisotropic (*s*-wave) pattern appeared to be modified by the underlying symmetry character. This is evidenced by a strongly pronounced line of maxima along the Fermi line, $\xi_{\mathbf{k}} = 0$, which closely reflected the anisotropic \mathbf{k} -dependence of the interlayer tunneling amplitude. Such a structure is both qualitatively and quantitatively in agreement with the available ARPES gap measurements in Bi2212⁶ and recent phenomenological gap calculations starting from the multi-band structure of the bilayer compounds.⁵⁴ Moreover, it is essentially embedded in the \mathbf{k} -dependence of $T_J(\mathbf{k})$, whereas suitable tuning of the intralayer coupling parameters can produce an *s*-wave contribution which shifts the nodes of the gap function slightly away from the Γ –*M* direction ($k_x = k_y$), as reported for ARPES experiments in bilayer Bi2212 at a given hole content.⁶

The gap obtained within the interlayer pair-tunneling mechanism appears to us to be quite promising in explaining a number of unusual properties of the superconducting state, such as for instance the anomalous tunneling response observed in HTCS junctions.^{57,32} Within the present approach, such unusual properties are associated with sharp \mathbf{k} -space features of the gap due to the presence of the renormalized pair-susceptibility $\chi_{\mathbf{k}}/[1 - T_J(\mathbf{k})\chi_{\mathbf{k}}]$.

The role of the interlayer tunneling mechanism in enhancing the value of the critical temperature for the normal-to-superconducting instability,¹⁹ as produced by a purely 2*D* correlation, has been discussed and generalized for a general doping level, qualitatively reproducing the universal non-monotonic dependence of T_c on the hole content.⁷³

The issue of the competition in the symmetry character of the gap function has been addressed both numerically and analytically in the context of the interlayer pair-tunneling mechanism. We were able to verify that in the presence of an interlayer pair-tunneling matrix element, the gap symmetry is pure and cannot be mixed on an underlying square lattice, at the critical point. The gap symmetry belongs to *one* of the irreducible representations of C_{4v} , and cannot be expressed as a linear combination of several basis functions of such irreducible representations. The one exception to this is when the

chemical potential is fine-tuned to a value such that accidental degeneracies occur. At exactly the critical point, moreover, the full \mathbf{k} -dependence and the critical exponent of the OP can be derived analytically, thus exhibiting its unconventional \mathbf{k} -space sharp structure and symmetry properties.

At temperatures well below T_c , and for certain filling fractions, mixing of symmetry channels may occur. We studied the location and width of the (μ, T) region allowing a mixed symmetry superconducting ground state on varying the coupling parameters and interlayer tunneling amplitude. In particular, we recovered prevalence of *s*-wave (resp., *d*-wave) symmetry at low (resp., high) band filling. This is due to the fact that the *symmetry* of the gap is determined by the dominant intralayer pairing symmetry, or equivalently the dominant intralayer dimensionless coupling constant. The “symmetry-projected” single-particle densities of states of this problem are such that *s*-wave coupling constant dominates at low band-filings, while *d*-wave coupling constants always dominate close to half-filling¹⁷. Both *s*-wave and *d*-wave symmetries are enhanced by increasing the inter-site attraction, whereas *s*-wave superconductivity is disfavored by increasing the on-site repulsion. However, the DOS argument given above also shows that the symmetry of the superconducting order parameter is highly dependent on doping.

Finally, we outlined how the solution to the gap equation can be employed in evaluating several quantities of interest. In particular, we have focussed our attention to entropy and the specific heat anomalies of the model at the critical point. The entropy in the superconducting state is found to have a temperature variation very similar to any conventional superconductor, mainly due to the fact that it is given by a \mathbf{k} -space integral over smooth functions involving the gap. The specific heat is found to have two unusual features. Firstly, for certain filling fractions, a mixing of symmetries may occur at a low temperature $T = T_m$, leading to an anomaly in the specific heat, *not associated with any true phase-transition*. Secondly, there is an anomaly at the superconducting transition $T = T_c$, for which our mean-field description is argued to give a reasonable description on the slightly overdoped side. This anomaly is analogous to the well-known step-discontinuity found in BCS, but in our case shows a novel feature. The normalized discontinuity turns out to be *not* a universal number, not only due to the different possible symmetries at the critical point, but also depending on the value of T_J , and is thus a manifestation of the unusual pairing kernel in the gap equation.

ACKNOWLEDGMENTS

Useful discussions with P. Falsaperla, J.O. Fjærstad, A.K. Nguyen, J. Nyhus, and E. Otnes are gratefully ac-

nowledged. One of the authors (G.G.N.A.) also thanks the NTNU for warm hospitality during a visiting term in Trondheim, and the Istituto Nazionale di Fisica Nucleare for financial support. One of the authors (A.S.) thanks the Norwegian Research Council for financial support under Grants No. 110566/410 and 10569/410.

APPENDIX A: NUMERICAL SOLUTION OF THE GAP EQUATIONS

For any fixed value of the chemical potential μ and temperature T , as well as of the coupling parameters λ_η and interlayer tunneling amplitude T_J , the gap parameters Δ_η are randomly initialized, and the nonlinear equation (13) is solved for $\Delta_{\mathbf{k}}$, for each wave-vector \mathbf{k} belonging to a suitably chosen fine mesh over the irreducible sector of the first Brillouin zone, $\{\mathbf{k} : 0 \leq k_x \leq \pi, 0 \leq k_y \leq k_x\}$. The values of $\Delta_{\mathbf{k}}$ thus obtained are employed to evaluate $M_{\eta\eta'}$ through Eq. (16). Equation (15) eventually defines the values of Δ_η , to be used at the successive steps in the iteration procedure. The iterative procedure terminates when self-consistency is achieved to within a preset tolerance limit in $|\Delta_{\mathbf{k}}|$. Special care had to be used near the nodes of the gap function. We verified the stability of the convergence procedure against the initial choice of Δ_η , and also by varying the number of \mathbf{k} -points in the mesh employed in the integrations.

High accuracy and a reasonably small computation time in the integration understood in Eq. (16), and elsewhere in the present paper, is made possible by using an adaptation to the 2D case of the analytical tetrahedron method.⁷⁰ An adaptive routine is suitable, due to the rapid variation of $\tilde{\chi}_{\mathbf{k}}$ in Eq. (16) for \mathbf{k} belonging to the locus defined by $\xi_{\mathbf{k}} = 0$ (i.e., the Fermi surface for noninteracting electrons). We carefully checked these routines by comparing the numerically evaluated DOS with available exact expressions.^{17,38}

APPENDIX B: GAP PARAMETERS AT THE MIXING TEMPERATURE

Following a procedure analogous to that outlined in Sec. IV B, one is able to derive a critical exponent 1/2 also for the gap components Δ_η which open at the mixing temperature $T = T_m$, thus endowing the gap function with an additional contribution with a generic h -wave symmetry, orthogonal to the one already present. Such a result is consistent with the conventional case ($T_J \rightarrow 0$), and is illustrated by the numerical example shown in Fig. 1. The calculations are more involved, although straightforward, and will not be shown here in detail. They must however take into account that a gap is *already* open at $T = T_m$. Generalizing the notation introduced in Sec. IV B, the final result is:

$$|\Delta_\eta| = \gamma_h \frac{T_m}{2} \left(1 - \frac{T}{T_m}\right)^{1/2} W_{\bar{\eta}\eta}^m, \quad (\text{B1})$$

where

$$\gamma_h^2 = \frac{1}{C_{\lambda_h}^m} \sum_{\eta\eta'}^h \lambda_\eta H_{\eta\eta'}^m W_{\eta\eta'}^m, \quad (\text{B2})$$

and

$$\begin{aligned} C_{\lambda_h}^m &= \frac{1}{N} \sum_{\mathbf{k}} \frac{\phi(\beta_m E_{\mathbf{k}}^m / 2)}{[1 - T_J(\mathbf{k}) \chi_{\mathbf{k}}^m]^3} \\ &\times \left\{ 1 - T_J(\mathbf{k}) \left[\chi_{\mathbf{k}}^m - 2\beta_m^3 \phi \left(\frac{1}{2} \beta_m E_{\mathbf{k}}^m \right) |\Delta_{\mathbf{k}}|^2 \right] \right\}^{-1} \\ &\times \left(\sum_{\eta\eta'}^h \lambda_\eta g_\eta(\mathbf{k}) W_{\eta\eta'}^m g_{\eta'}(\mathbf{k}) \right) \\ &\times \left(\sum_{\eta}^h W_{\bar{\eta}\eta}^m g_\eta(\mathbf{k}) \right)^2, \end{aligned} \quad (\text{B3})$$

$$\begin{aligned} H_{\eta\eta'}^m &= \frac{1}{N} \sum_{\mathbf{k}} \frac{g_\eta(\mathbf{k}) g_{\eta'}(\mathbf{k})}{[1 - T_J(\mathbf{k}) \chi_{\mathbf{k}}^m]^2} \left[\operatorname{sech}^2 \left(\frac{1}{2} \beta_m E_{\mathbf{k}}^m \right) \right. \\ &\left. + 4\beta_m \phi \left(\frac{1}{2} \beta_m E_{\mathbf{k}}^m \right) \left(\frac{\partial |\Delta_{\mathbf{k}}|^2}{\partial T} \right)_{T=T_m+0} \right]. \end{aligned} \quad (\text{B4})$$

An index m denotes the inclusion of the gap function without the new h -wave contribution, and that the limit $T \rightarrow T_m$ has been taken afterwards.

The above equations reduce to the analogous ones derived in Sec. IV B at $T = T_c$ and $\Delta_{\mathbf{k}} = 0$. The latter expressions are analytical but not in closed form, since they require the knowledge of $\beta(\partial|\Delta_{\mathbf{k}}|^2/\partial T)$, at $T = T_m + 0$, which can be accessed only numerically. However, one expects such quantity to be vanishingly small for $T_m \ll T_c$, like in the conventional case. (It would be exactly zero if $T_m = 0$).

¹ P.W. Anderson, Science **256**, 1526 (1992).

² Ch.P. Poole, Jr., H.A. Farach, and R.J. Creswick, *Superconductivity* (Academic Press, San Diego, 1995).

³ H. Srikanth, B.A. Willemse, T. Jacobs, S. Sridhar, A. Erb, E. Walker, and R. Fükiger, Phys. Rev. B **55**, R14733 (1997).

⁴ H. Srikanth, Z. Zhai, S. Sridhar, A. Erb, and E. Walker, preprint cond-mat/9709085 (unpublished).

⁵ M. Randeria and J.C. Campuzano, in *Models and phenomenology for conventional and high-temperature superconductivity. Proceedings of the CXXXVI International School of Physics “E. Fermi”*, edited by G. Iadonisi, R.J. Schrieffer, and M.L. Chiofalo (IOS, Amsterdam, 1998).

- ⁶ H. Ding, J.C. Campuzano, A.F. Bellman, T. Yokoya, M.R. Norman, M. Randeria, T. Takahashi, H. Katayama-Yoshida, T. Mochiku, K. Kadowaki, and G. Jennings, Phys. Rev. Lett. **74**, 2784 (1995), [**75**, 1425 (1995)].
- ⁷ B.G. Levi, Phys. Today **46**, 17 (1993).
- ⁸ B.E.C. Koltenbah and R. Joynt, Rep. Prog. Phys. **60**, 23 (1997).
- ⁹ D.A. Wollman, D.J. Van Harlingen, W.C. Lee, D.M. Ginsberg, and A.J. Legget, Phys. Rev. Lett. **71**, 2134 (1993).
- ¹⁰ D.A. Wollman, D.J. Van Harlingen, W.C. Lee, D.M. Ginsberg, and A.J. Legget, Phys. Rev. Lett. **73**, 1872 (1994).
- ¹¹ D.A. Wollman, D.J. Van Harlingen, J. Giapintzakis, and D.M. Ginsberg, Phys. Rev. Lett. **74**, 797 (1995).
- ¹² C.C. Tsuei, J.R. Kirtley, C.C. Chi, L.S. Yu-Jahnes, A. Gupta, T. Shaw, J.Z. Sun, and M.B. Ketchen, Phys. Rev. Lett. **73**, 593 (1994).
- ¹³ T. Schneider, H. De Raedt, and M. Frick, Z. Phys. B, **76**, 3 (1989); H. De Raedt, T. Schneider, and M.P. Sørensen, *ibid.* **79**, 327 (1990); T. Schneider and M.P. Sørensen, *ibid.* **80**, 331, (1990); **81**, 3 (1990).
- ¹⁴ P.N. Spathis, M.P. Soerensen, and N. Lazarides, Phys. Rev. B **45**, 7360 (1992).
- ¹⁵ Q.P. Li, B.E.C. Koltenbah, and R. Joynt, Phys. Rev. B **48**, 437 (1993).
- ¹⁶ C. O'Donovan and J.P. Carbotte, Physica C **252**, 87 (1995).
- ¹⁷ E. Otnes and A. Sudbø, preprint cond-mat/9707225 (unpublished).
- ¹⁸ J.M. Wheatley, T. Hsu, and P.W. Anderson, Phys. Rev. B **37**, 5897 (1988).
- ¹⁹ S. Chakravarty, A. Sudbø, P.W. Anderson, and S. Strong, Science **261**, 337 (1993).
- ²⁰ P.W. Anderson, *The Theory of Superconductivity in the High- T_c Cuprates* (Princeton Series in Physics, Princeton, 1997).
- ²¹ S.L. Cooper, P. Nyhus, D. Reznik, M.V. Klein, W.C. Lee, D.M. Ginsberg, B.W. Veal, A.P. Paulikas, and B. Dabrowski, Phys. Rev. Lett. **70**, 1533 (1993).
- ²² S. Uchida, K. Tamasaku, and S. Tajima, Phys. Rev. B **53**, 14558 (1996).
- ²³ P.W. Anderson, Physica B **199&200**, 8 (1994).
- ²⁴ D.G. Clarke, S.P. Strong, and P.W. Anderson, Phys. Rev. Lett. **72**, 3218 (1994).
- ²⁵ P.W. Anderson and D. Khveshchenko, Phys. Rev. B **52**, 16415 (1995).
- ²⁶ O.K. Andersen, S.Y. Savrasov, O. Jepsen, and A.I. Liechtenstein, J. Low Temp. Phys. **105**, 285 (1996).
- ²⁷ A. Sudbø, S. Chakravarty, S. Strong, and P.W. Anderson, Phys. Rev. B **49**, 12245 (1994).
- ²⁸ L. Yin, S. Chakravarty, and P.W. Anderson, Phys. Rev. Lett. **78**, 3559 (1997).
- ²⁹ A. Sudbø, J. Low Temp. Phys. **97**, 403 (1994).
- ³⁰ A. Sudbø and S.P. Strong, Phys. Rev. B **51**, 1338 (1995).
- ³¹ L. Yin and S. Chakravarty, Int. J. Mod. Phys. B **10**, 805 (1996).
- ³² G.G.N. Angilella, in preparation (unpublished).
- ³³ P.W. Anderson, Science **279**, 1196 (1998).
- ³⁴ S. Chakravarty, Europ. Phys. J., to be published. Preprint cond-mat/9801025 (unpublished).
- ³⁵ J. Yu and A.J. Freeman, Jour. Phys. Chem. of Solids **52**, 1351 (1991).
- ³⁶ Z.-X. Shen, D.S. Dessau, B.O. Wells, D.M. King, W.E. Spicer, A.J. Arko, D. Marshall, L.W. Lombardo, A. Kapitulnik, P. Dickinson, S. Doniach, J. DiCarlo, A.G. Loeser, and C.H. Park, Phys. Rev. Lett. **70**, 1553 (1993).
- ³⁷ A Van Hove singularity in the single particle DOS at the Fermi-surface corresponds to a second derivative of the free energy with respect to filling which is *negative*, i.e. an unstable situation with a local maximum in the free energy. The way a system avoids such a situation when the Fermi-level approaches a Van Hove singularity, is through reconstruction of the underlying lattice. This splits a 2D logarithmic singularity into two singularities, such that the Fermi-level is located at a local minimum in the DOS in between the new singularities. Note that the fact that high- T_c superconductors *self-dope* to optimum filling clearly negates the notion that optimum doping corresponds to an unstable situation with a local maximum in the free energy.
- ³⁸ D.Y. Xing, M. Liu, and C.D. Gong, Phys. Rev. B **44**, 12525 (1991).
- ³⁹ I.S. Gradshteyn and I.M. Ryzhik, *Table of Integrals, Series, and Products* (Academic Press, San Diego, 1980).
- ⁴⁰ J.F. Annett and R.M. Martin, Phys. Rev. B **42**, 3929 (1990).
- ⁴¹ M.R. Norman, M. Randeria, H. Ding, and J.C. Campuzano, Phys. Rev. B **52**, 615 (1995).
- ⁴² On the other hand, it may be worth emphasizing that the physical origin of in-plane pairing is logically independent from the ILPT mechanism, as earlier recognized by Anderson (see, e.g., Ref. 20).
- ⁴³ J.F. Annett, Adv. Phys. **39**, 83 (1990).
- ⁴⁴ D.J. Scalapino, Phys. Rep. **250**, 329 (1995).
- ⁴⁵ It is understood that normal Hartree terms, i.e. of the form $\propto c_{\mathbf{k}\downarrow}^{i\dagger} c_{\mathbf{k}'\uparrow}^j \langle c_{-\mathbf{k}\downarrow}^{i\dagger} c_{-\mathbf{k}'\downarrow}^j \rangle$, can be absorbed in the renormalization of the chemical potential, which is here treated as a free parameter.
- ⁴⁶ P. Fischer, H.W. Neumüller, B. Roas, H.F. Braun, and G. Saemann-Ischenko, Solid State Commun. **72**, 871 (1989).
- ⁴⁷ M. Sigrist and K. Ueda, Rev. Mod. Phys. **63**, 239 (1991).
- ⁴⁸ F. Siringo, G.G.N. Angilella, and R. Pucci, Phys. Rev. B **53**, 2870 (1996).
- ⁴⁹ A.A. Abrikosov, Physica C **244**, 243 (1995).
- ⁵⁰ C. O'Donovan and J.C. Carbotte, Physica C **252**, 87, (1995); Phys. Rev. B, **52**, 4568 (1995); *ibid.* **52**, 16208 (1995).
- ⁵¹ G.G.N. Angilella, Ph.D. thesis, University of Catania, 1999.
- ⁵² Note that it is the presence of a generally nonzero $\Delta_{\mathbf{k}}$ in the pair susceptibility $\chi_{\mathbf{k}}$ which prevents the quantity $1 - T_J(\mathbf{k})\chi_{\mathbf{k}}$ from being actually zero for $T < T_c$.
- ⁵³ A. Perali, C. Castellani, C. Di Castro, and M. Grilli, Phys. Rev. B **54**, 16216 (1996).
- ⁵⁴ W.M. Temmermann, Z. Szotek, B.L. Gyorffy, O.K. Andersen, and O. Jepsen, Phys. Rev. Lett. **76**, 307 (1996).
- ⁵⁵ M.R. Norman, M. Randeria, H. Ding, and J.C. Campuzano, preprint cond-mat/9711232 (unpublished).
- ⁵⁶ Ch.P. Enz, *A Course on Many-Body Theory Applied to Solid State Physics* (World Scientific, Singapore, 1992).

- ⁵⁷ J.Y.T. Wei, C.C. Tsuei, P.J.M. van Bentum, Q. Xiong, C.W. Chu, and M.K. Wu, Phys. Rev. B **57**, 3650 (1998).
- ⁵⁸ J.O. Fjærrestad and A. Sudbø, in preparation (unpublished).
- ⁵⁹ G.G.N. Angilella, R. Pucci, and F. Siringo, Phys. Rev. B **54**, 15471 (1996).
- ⁶⁰ A. A. Abrikosov, L. P. Gor'kov, and I. E. Dzyaloshinski, *Methods of quantum field theory in statistical physics* (Dover Publications, Inc., New York, 1963).
- ⁶¹ R. Fehrenbacher and M.R. Norman, Phys. Rev. Lett. **74**, 3884 (1995).
- ⁶² A. Sudbø, Physica C **235**, 126 (1994).
- ⁶³ P.W. Anderson, J. Phys. Chem. Solids **56**, 1593 (1995), proceedings of the Conference on Spectroscopies in Novel Superconductors. Stanford, CA, March 15-18, 1995.
- ⁶⁴ M.R. Norman, H. Ding, M. Randeria, J.C. Campuzano, T. Yokoya, T. Takeuchi, T. Takahashi, T. Mochiku, K. Kadowaki, P. Guptasarma, and D.G. Hinks, Nature **392**, 157 (1998).
- ⁶⁵ S. Strong and P.W. Anderson, Chinese Journal of Physics **34**, 159 (1996).
- ⁶⁶ M. Tinkham, *Superconductivity* (McGraw-Hill, Inc., New York, 1996), second Edition.
- ⁶⁷ N. Bulut and D.J. Scalapino, Phys. Rev. Lett. **68**, 706 (1992).
- ⁶⁸ Q. P. Li and R. Joynt, Phys. Rev. B **47**, 530 (1993).
- ⁶⁹ A.J. Leggett, Rev. Mod. Phys. **47**, 331 (1995).
- ⁷⁰ P. Lambin and J.P. Vigneron, Phys. Rev. B **29**, 3430 (1984).
- ⁷¹ R. Movshovich, M.A. Hubbard, M.B. Salamon, A.V. Balatsky, R. Yoshizaki, and J.L. Sarrao, preprint cond-mat/9709061 (unpublished).
- ⁷² A. K. Nguyen and A. Sudbø, Phys. Rev. B **57**, 3123 (1998).
- ⁷³ H. Zhang and H. Sato, Phys. Rev. Lett. **70**, 1697 (1993); H. Zhang, H. Sato, and G.L. Liedl, Physica C, **234**, 185 (1994).

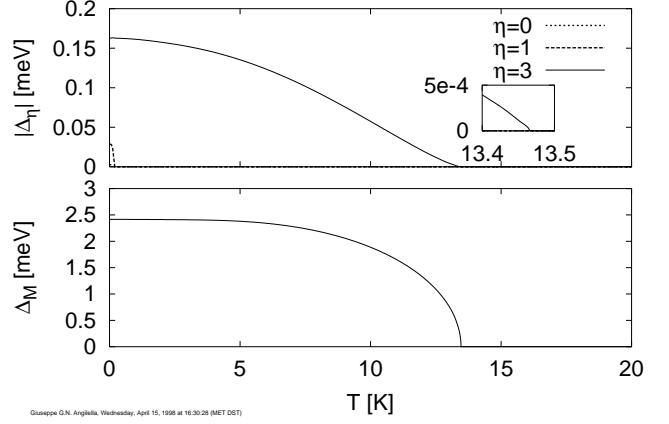


FIG. 1. Temperature dependence of the gap parameters $|\Delta_\eta|$ (top), and of the gap maximum Δ_M (bottom), at $\mu = -0.4850$ eV. Chosen values of the in-plane coupling parameters and of the interlayer tunneling amplitude are $\{\lambda_0, \lambda_1, \lambda_2, \lambda_3, \lambda_4\} = \{0.01, -0.2125, 0.0, -0.2125, 0.0\}$ eV and $t_\perp = 0.08$ eV, respectively, yielding a critical temperature $T_c \approx 13.4$ K, at which Δ_k opens with d -wave symmetry, and a mixing temperature $T_m \approx 0.2$ K, where Δ_k acquires an s -wave contribution. The inset in the top figure shows that Δ_3 displays the expected critical behavior, with critical exponent $1/2$, only very close to T_c .

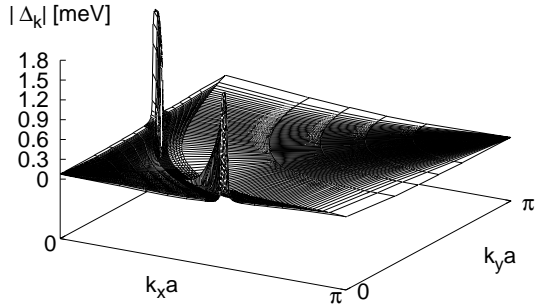
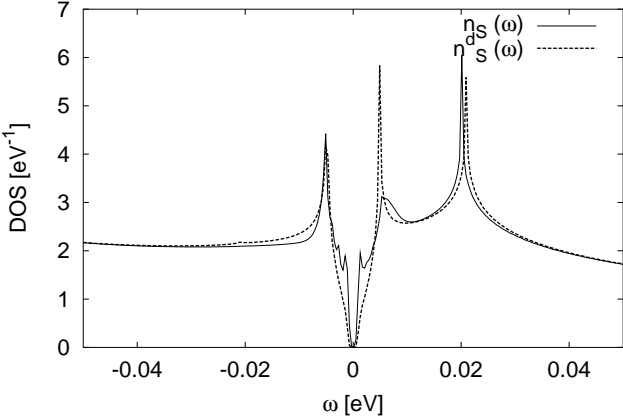


FIG. 2. Dependence of $|\Delta_k|$ over the \mathbf{k} in the first quarter of the 1BZ, at $\mu = -0.4892$ eV and $T = 0$. Same values of the parameters as in Fig. 1. Notice the maxima structure along the $\xi_k = 0$ locus, including peaks at the intersection thereof with $k_y = 0$ and $k_x = \pi/a$, and symmetry related points, whose height is enhanced as T decreases, due to the prefactor $[1 - T_J(\mathbf{k})\chi_{\mathbf{k}}]^{-1}$ in Eq. (12).



Giuseppe G.N. Angilella, Thursday, February 26, 1998 at 17:42:06 (MET)

FIG. 3. Superconducting DOS $n_S(\omega)$, corresponding to an anisotropic \mathbf{k} -dependent gap in the presence of ILPT (continuous line), and $n_S^d(\omega)$, corresponding to a purely d -wave gap, without ILPT (dashed line), at $\mu = -0.47$ eV, $T = 0$ K. Same values of the parameters as in Fig. 1.

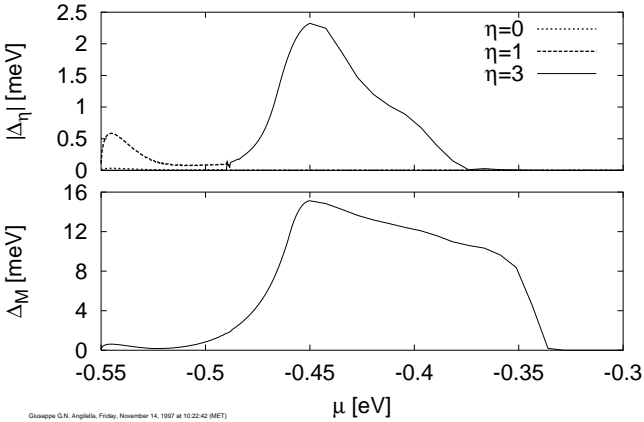
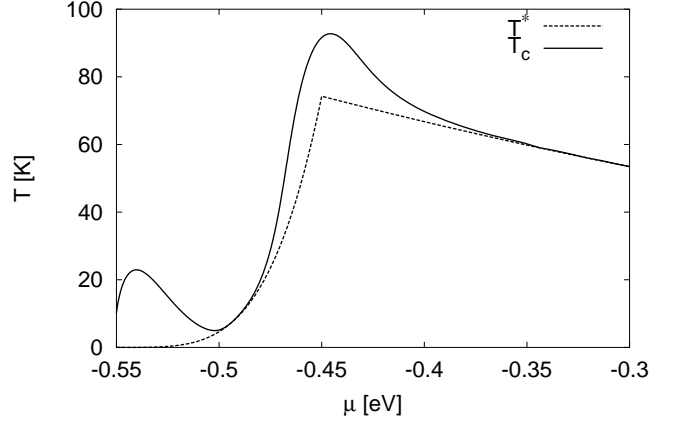
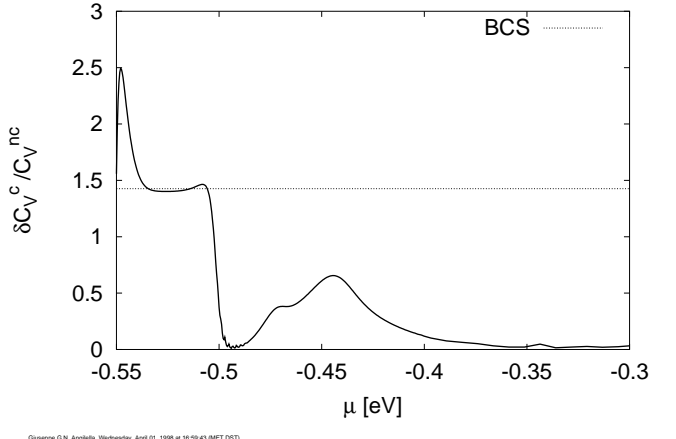


FIG. 4. Dependence of the gap parameters $|\Delta_\eta(T = 0)|$ and of the gap maximum at zero temperature Δ_M on the chemical potential μ . Same values of the parameters as in Fig. 1.



Giuseppe G.N. Angilella, Wednesday, April 01, 1998 at 15:51:27 (MET DST)

FIG. 5. Lower bound temperature $T^*(\mu)$ (dashed line) and critical temperature $T_c(\mu)$ (continuous line), as functions of the chemical potential μ . Same values of the parameters as in Fig. 1.



Giuseppe G.N. Angilella, Wednesday, April 01, 1998 at 16:59:43 (MET DST)

FIG. 6. Normalized jump $\delta C_V^c / C_V^{nc}$ in the specific heat at $T = T_c$ within the ILPT mechanism, as a function of the chemical potential μ (continuous line). Like in Fig. 1, we used $\{\lambda_0, \lambda_1, \lambda_2, \lambda_3, \lambda_4\} = \{0.01, -0.2125, 0.0, -0.2125, 0.0\}$ eV and $t_\perp = 0.08$ eV, respectively. The BCS universal limit $12/[7\zeta(3)] \simeq 1.42613$ is also shown, for comparison (dashed line).